

PEOPLE'S DEMOCRATIC REPUBLIC OF ALGERIA
MINISTRY OF HIGHER EDUCATION AND SCIENTIFIC RESEARCH

IBN-KHALDOUN UNIVERSITY OF TIARET

FACULTY OF APPLIED SCIENCES
DEPARTMENT OF ELECTRICAL ENGINEERING



Final year project for the master's degree

Domain: Science and Technology

Branch: Electrical engineering

Option: Electrical controls

THEME

**Performance evaluation of the application of
the genetic algorithm for tracking the
maximum power point of a photovoltaic
system**

Prepared by: ZEGAI Amina

BOUCHEDJRA Sara

Examination Board

First and last name	Grade	Quality
Belfedal Cheikh	Pr	President
Belabbas Belkacem	MCA	Supervisor
Allaoui Tayeb	Pr	Co-supervisor
Mihoub Youcef	MCA	Examiner
Tahri ahmed	MCB	Examiner
Benabdallah Naima	Phd	invited

Academic year : 2024/2025

Acknowledgements

First and foremost, we thank **Allah**, the Almighty, for granting us the strength, patience, and perseverance needed to carry out this work.

We extend our sincere thanks to the members of the jury, especially **Mr. Belfedal Cheikh**, President of the jury, as well as **Mr. Mihoub Youcef** and **Mr. Tahri Ahmed**, for the honor they have given us by evaluating this thesis and for their valuable and enriching comments.

Our heartfelt thanks go to our supervisors **Mr. Belabbas Belkacem** and **Mr. Allaoui Tayeb** for their invaluable advice, attentive support and relevant guidance throughout this project.

We would also like to warmly thank **Ms. Benabdallah Naima** for her valuable assistance, kindness, and technical advice, which greatly helped us at every stage of this work. Her availability and willingness to share her knowledge were of great support.

We also express our gratitude to all the teachers in the Department of Electrical Engineering for the knowledge they imparted during our academic journey. Special thanks to the members of the Laboratory **L2GEGI** for their valuable assistance and the time they kindly devoted to us.

Finally, we sincerely thank our families for their unwavering support, encouragement, and patience, and to our classmates for their collaboration, motivation, and the positive spirit shared throughout this experience.



Dedication

To our mothers, for their unconditional love, silent sacrifices, and unwavering support.

To our fathers, for their wisdom, hard work, and constant presence by our side.

To our brothers and sisters, for their affection, patience, and encouragement throughout this journey.

To our friends, for their solidarity, support, and the moments we shared during this experience.

And to all those who helped us, directly or indirectly, we express our deep gratitude.



LIST OF FIGURES	
LIST OF TABLES	
NOMENCLATURES.....	
LIST OF ACRONYMS.....	
GENERAL INTRODUCTION.....	1

Chapter I: Photovoltaic solar energy and MPPT control techniques

I.1 INTRODUCTION	5
I.2 TYPES OF RENEWABLE ENERGY	5
I.3 SOLAR ENERGY	6
I.4 PHOTOVOLTAIC ENERGY	7
I.4.1 History of photovoltaic energy	8
I.5 PHOTOVOLTAIC CELLS	8
I.5.1 Principle of cell operation.....	9
I.6 ADVANTAGES AND DISADVANTAGES OF PHOTOVOLTAIC ENERGY.....	10
I.6.1 Advantages of photovoltaic energy	10
I.6.2 Disadvantages of photovoltaic energy	10
I.7 DC-DC CONVERTERS	11
I.8 TYPES OF DC-DC CONVERTERS USED IN PHOTOVOLTAIC SYSTEMS.....	11
I.9 THE MPPT CONTROL	12
I.10 CLASSIFICATION OF MPPT CONTROLLERS.....	12
I.10.1 Conventional methods	12
I.10.2 Non-conventional (intelligent) methods	13
I.11 THE PERTURB AND OBSERVE (P&O) METHOD	13
I.12 ARTIFICIAL NEURAL NETWORKS	14
I.12.1 History	14
I.12.2 Biological foundation	15
I.12.2.1 Biological basis.....	15
I.12.3 mathematical model (artificial neuron).....	16
I.12.3.1 Activation Function	17
I.12.4 Neural Network Architecture.....	18
I.12.4.1 Non-looped networks.....	18
I.12.4.2 Looped networks	19
I.13 GENETIC ALGORITHMS	19
I.13.1 Basic definitions of genetic algorithms.....	19
I.13.2 History and principle	20
I.13.3 The coding	21
I.13.4 Generation of the initial population	21
I.13.4.1 Evaluation (fitness).....	21
I.13.4.2 Genetic Operations	22
I.14 PARTIAL SHADING.....	22
I.14.1 Causes of shading	23
I.14.2The partial shading effect	23
I.14.3 By-pass diode for a photovoltaic solar module.....	24
I.15 CONCLUSION.....	24

Chapter II: Dynamic Simulation and Optimization of PV Systems with MPPT Control

II.1 INTRODUCTION	26
II.2 MODELING OF A PHOTOVOLTAIC CELL.....	26
II.2.1 Presentation and simulation of the PV module:	27
II.2.2 Influence of temperature on the PV cell.....	29
II.2.3 Influence of irradiance on the PV cell	30

II.3 MODELING OF A DC-DC BOOST CONVERTER	31
II.3.1 Operation	32
II.3.2 Equivalent mathematical model	32
II. 4 MPPT CONTROL	33
II.4.1 MPPT principle	34
II.4.2 Perturb & Observe (P&O) Method	34
II.4.3 Perturb & Observe (P&O) Simulation:	35
II.4.4 Simulation results	36
II.5 CONCLUSION	39
Chapter III: ANN and GA-Based MPPT Under Varying and Shaded Conditions	
III.1 INTRODUCTION	41
III.2 ANN-BASED MPPT ALGORITHM	41
III.2.1 Principle of training ANN-based MPPT algorithm	41
III.2.2 Artificial neural network (ANN) simulation	42
III.2.3 Simulation results	43
III.3 GAS-BASED MPPT ALGORITHM:	47
III.3.1 Genetic algorithms (GA) simulation	48
III.3.2 Simulation results	48
III.4 PARTIAL SHADING BASED MPPT ALGORITHMS	51
III.4.1 Testing partial shading model	51
III.5 COMPARATIVE PERFORMANCE STUDY	52
III.5.1 Under normal conditions	53
III.5.2 Under partial shading	55
III.5 CONCLUSION	58
Chapter IV: Experimental Validation of MPPT Control for PV Systems Using dSPACE	
IV.1 INTRODUCTION	60
IV. 2 PRESENTATION OF DSPACE 1104	60
IV.2.1 dSPACE 1104 Inputs/Outputs	60
IV.2.2 Control Desk	61
IV.3 REALIZATION OF THE ELECTRONIC CIRCUIT	62
IV.4 REALIZATION RESULTS	63
IV.4.1 Test of Boost converter	64
IV.4.2 Implementation of the P&O algorithm	64
IV.5 CONCLUSION	65
General conclusion	67
Annexes	69
Bibliographical References	73

List of figures

Chapitre I

Figure I. 1 : Types of renewable energy.[4].....	6
Figure I. 2: Photovoltaic solar energy.[5]	6
Figure I. 3 : Solar radiation.[6]	7
Figure I. 4 : Photovoltaic cells. [9]	9
Figure I. 5 : Principle of a photovoltaic cell.[10].....	10
Figure I. 6 : Symbol of DC-DC converter. [12].....	11
Figure I. 7 : Characteristic P_{pv} (V_{pv}) P&O.[14]	14
Figure I. 8: Biological neuron.[17]	15
Figure I. 9: Artificial neuron model [19]	17
Figure I. 10: Non-looped networks.[21]	18
Figure I. 11: Looped networks.[23]	19
Figure I. 12 : Partial shading of photovoltaic panels . [30].....	23
Figure I. 13 : PV system under partially shaded conditions caused by passing clouds.[31]	23
Figure I. 14 : Use of the by-pass diode.[33]	24

Chapitre II

Figure II. 1 : Equivalent model of the PV cell.....	26
Figure II. 2: I-V characteristics of PV under standard conditions.	28
Figure II. 3: P-V characteristics of PV under standard conditions.	29
Figure II. 4: Influence of temperature On the I_V characteristics.	29
Figure II. 5: Influence of temperature On the P_V characteristics.	30
Figure II. 6: Influence of irradiance on The I_V characteristics.....	30
Figure II. 7: Influence of irradiance on The P_V characteristics.	31
Figure II. 8: Topology of a DC-DC Boost converter.....	31
Figure II. 9: Electrical diagram of a closed boost converter.	32
Figure II. 10: Electrical diagram of an open boost converter.	33
Figure II. 11: Solar energy conversion chain with MPPT control. [5]	34
Figure II. 12: The flowchart of the P&O Algorithm.....	35
Figure II. 13: Simulation diagram of P&O algorithm.....	35
Figure II. 14: Irradiance variations.	36
Figure II. 15: Temperature variations.....	36
Figure II. 16: Tracking of MPP current by P&O.	37
Figure II. 17: Tracking of MPP voltage by P&O.	37
Figure II. 18: Tracking of MPP power by P&O.	37
Figure II. 19: Tracking of MPP duty cycle by P&O.....	38

Chapitre III

Figure III. 1: Flowchart of the training process of the ANN for MPPT.....	42
Figure III. 2 : Architecture of the proposed ANN.	43
Figure III. 3 : The general diagram of ANN algorithm.	43
Figure III. 4 :Performance plot of the ANN training.....	44
Figure III. 5 : Simulink bloc of the trained ANN MPPT.....	44
Figure III. 6 : Tracking of MPP current by ANN.....	45
Figure III. 7 : Tracking of MPP voltage by ANN.	45
Figure III. 8 : Tracking of MPP power by ANN.	45
Figure III. 9 : Tracking of MPP duty cycle by ANN.....	46
Figure III. 10 : GAs-based MPPT system. [5].....	47
Figure III. 11 : Flow chart of GAs-based MPPT.....	47
Figure III. 12 : The general diagram of GAs algorithm.	48
Figure III. 13 : Tracking of MPP current by GA.....	49
Figure III. 14 : Tracking of MPP voltage by GA.	49
Figure III. 15 : Tracking of MPP power by GA.....	49

Figure III. 16 : Tracking of MPP duty cycle by GA..... 50
Figure III. 17 : Partial shading test setup..... 51
Figure III. 18: I-V characteristics of PV under partial shading 52
Figure III. 19: P-V characteristics of PV under partial shading 52
Figure III. 20 : PV voltage comparaisn under normal conditions. 53
Figure III. 21 : PV current comparison under normal conditions..... 53
Figure III. 22 : PV power comparison under normal conditions. 54
Figure III. 23 : Instantaneous MPPT tracking error under normal conditions..... 54
Figure III. 24 : PV voltage comparison under partial shading conditions. 55
Figure III. 25 : PV current comparison under partial shading conditions. 56
Figure III. 26 : PV power comparison under partial shading conditions. 56
Figure III. 27 : Instantaneous MPPT tracking error under partial shading. 57

Chapitre IV

Figure IV. 1 : Connection panel for DSPACE 1104. 60
Figure IV. 2 : Construction of the dSPACE 1104 serial interface. 61
Figure IV. 3 : Control Desk interface. 62
Figure IV. 4 : DIMEL SOLAR Panel. 62
Figure IV. 5 : The experimental PV system..... 63
Figure IV. 6 : Electrical Response of the Converter During Testing..... 64
Figure IV. 7 : Experimental Results of P&O Algorithm Implementation. 65

List of tables

<i>Chapitre I</i>	
Table I. 1: Function of the biological neuron.[17]	16
Table I. 2: Activation functions [15].....	18
<i>Chapitre II</i>	
Table II. 1: Electrical characteristics of the photovoltaic panel.	28
Table II. 3: Electrical characteristics of the DC-DC Boost converter.	32
<i>Chapitre III</i>	
Table III. 1: Comparative performance study of MPPT techniques.	58
<i>Chapitre IV</i>	
Table IV. 1 : Components of realization	63

Nomenclatures

R_s : Series resistance .

R_{sh} : Shunt resistance .

V_{oc} : Open circuit voltage .

I_{sc} : Short-circuit current .

I_{ph} : Photocurrent .

I_{pv} : Photovoltaic current .

V_{pv} : Photovoltaic voltage .

I_d : Current flowing through the diode .

I_{sh} : Current flowing through the shunt resistor R_{sh} .

V_t : Thermal voltage .

n : Ideality factor of the diode .

q : Electronic charge ($1.602 \cdot 10^{-19} \text{ c}$) .

k : Boltzman constant ($1.381 \cdot 10^{-23} \text{ j/k}$) .

G : Irradiance .

G_n : Nominal irradiance .

T : Temperature .

T_n : Nominal temperature .

I_s : Reverse saturation current at T_n .

I_{rs} : Reverse saturation current at T .

K_i : Temperature coefficient of short-circuit current, [A/K] or [A/C°].

N_{pp} : Parallel cells .

N_{ss} : Series cells .

E_g : Bandgap energy (ev) .

V : Result of the sum .

Q : Activation function .

Y : Output .

X : Vector of inputs .

W : Neuron's vector of weights .

b : Bias .

T_{sel} : Selection rate .

V_i : Input voltage .

V_o : Output voltage .

P_{max} : Maximum power .

V_{mp} : Voltage at P_{max} .

I_{mp} : Current at P_{max} .

List of acronyms

PV : Photovoltaic .

DC : Direct current .

MPP : Maximum power point .

MPPT : Maximum power point tracking .

P&O : Perturb and observe .

GA : Genetic algorithm .

ANN : Artificial neural network .

AI : Artificial intelligence .

DC- DC : Direct current- Direct current .

MSE : Mean Square Error .

PWM : Pulse Width Modulation .

DSP : Digital Signal Processor.

ADCs : Analog-to-digital converter .

DACs : Digital-to-analog converter .

LED : Light Emitting Diode .

BNC : Bayonet Neill Connector .

PC : Personal Computer .

DS : DSPACE .

General introduction

Renewable energies are emerging as a potential solution for reducing atmospheric pollution. When we say renewable, we mean energy generated from the sun, wind, heat from the earth, water and biomass. The type chosen for this contribution is photovoltaic (PV) energy.[1]

Solar energy is an attractive alternative to fossil fuel energy. The direct conversion of solar radiation into electricity is known as the photovoltaic effect. PV energy is developing very rapidly. undefined it is durable, clean and free of environmental pollution.[1]

Adapting the voltage and current levels of the elements of the electrical energy (solar panels, load, batteries, and networks) with respect to a DC bus requires a DC-DC static converter. In a photovoltaic system, the employed DC-DC converters are of the Buck, Boost, and Buck-Boost types. In our study, we focus on the Boost converter.

DC-DC static converters generate a adjusted DC voltage from a fixed DC voltage. The Boost converter acts as a voltage lifter, meaning that the input voltage will be increased thanks to the structure of this converter. It consumes little power and allows a very good efficiency.[2]

Depending on the electrical characteristics of the photovoltaic cells and their combination, the efficiency of PV systems can be improved by methods known as Maximum Power Point Tracking techniques. In most PV energy conversion systems, there is a particular algorithm known as MPPT. This technique, as the name suggests, is used to extract the maximum power that the panel is capable of delivering. The power required generally depends on changes in climatic conditions such as irradiance and temperature. Consequently, the MPPT technology, designed to control the duty cycle of the DC-DC boost converter , is required for optimum operation of the PV system under different operating conditions . [3]

Many MPPT methods have been proposed in the literature, such as the perturb and observe method (P&O), the hill climbing method (HC), and the incremental conductance method (INC). Intelligent control techniques have also been proposed to improve the performance of these methods. In particular, fuzzy logic, artificial neural networks. The choice of this solution is justified by the fact that artificial intelligence allows capturing the operator's know-how and system knowledge without necessarily relying on a mathematical model, which is not always easy to determine. The objective of this work is the application of intelligent control on MPPT, which will act on the duty cycle that will command the Boost converter for photovoltaic conversion.[2]

The phenomenon of shading in solar panels occurs when part of the panel is in the shade, reducing the efficiency of energy production due to the variation in illumination between

photovoltaic cells. This shading causes hot spots and makes it difficult to determine the maximum power point (MPP). However, it is crucial to think about developing strategies and approaches that enable the search for maximum power points to guarantee high-performance PV system operation corresponding to global max points, as opposed to the conventional algorithms available.[1]

The main objective of this work is to evaluate the performance of the genetic algorithm (GA) in tracking the maximum power point (MPP) of a photovoltaic system by comparing it with conventional method (P&O) and intelligent method (ANN).

The dissertation is organized into four chapters:

In the first chapter, we introduced photovoltaic systems. We presented the fundamental concepts of renewable energies, solar radiation, and photovoltaic cell operation, as well as their advantages and disadvantages. We then presented DC-DC converters and the various MPPT control techniques, whether conventional, such as Perturb and Observe (P&O), or intelligent, such as genetic algorithms (GA) and artificial neural networks (ANN). The chapter concludes with an analysis of the effect of partial shading, a major challenge for photovoltaic power optimization.

In the second chapter, we go a step further by modeling photovoltaic systems and analyzing their electrical characteristics. We also present the influence of climatic conditions (temperature and irradiation) on the behavior of photovoltaic systems. We then move on to modeling the Boost converter, which plays an essential role in adapting the system's output voltage. We study the MPPT control principle and its importance in optimizing power output. Finally, we simulate the PV system using the classic Perturb and Observe (P&O) method in the Matlab/SimPowerSystems environment.

The third chapter focuses on the study and simulation of intelligent maximum power point tracking (MPPT) methods, in particular artificial neural networks (ANNs) and genetic algorithms (GAs). Both approaches are presented with explanatory flowcharts, enabling step-by-step visualization of how they work. They are then implemented in the simulation to assess their performance under different conditions. A comparative study of the three MPPT methods (P&O, ANN, and AG) is carried out under normal and partial shading conditions. This comparison is based on several performance criteria, including stability, speed, and tracking efficiency. The results obtained are analyzed in detail.

The fourth chapter is devoted to the practical realization of a PV system based on the DSPACE 1104 card. We present the DSPACE 1104 card used to control PV systems, its inputs/outputs, and the programming environment (Control Desk). Next, preliminary tests were carried out on the

boost converter to verify its correct operation. The P&O method was implemented on the platform. Finally, the results of the PV system implementation based on a DSPACE 1104 card were analyzed.

The work concludes with a general conclusion.

Chapter I

Photovoltaic solar energy and MPPT control techniques

I.1 Introduction

Renewable energy (RE), as a sustainable and clean energy source, has multiple benefits for the environment and the economic sector. Based on the findings of the International Renewable Energy Agency (IRENA), RE is increasingly being recognized as a crucial avenue for deployment and a significant contributor to greenhouse gas reduction. The analysis reveals that over 90 % of carbon dioxide emissions have been successfully mitigated through the utilization of RE sources. In the future, RE will undoubtedly be the most promising source of electrical energy generation. This is due to its unlimited potential, eco-friendly nature, and sustainability. In relation to this, photovoltaic (PV) energy, as a direct application of solar energy has been known to have considerable attractiveness among other RE-based applications due to many merits, for example, cost-effective, without noise, ease of implementation, worldwide accessibility, and a minor maintenance requirement.[1]

Research into renewable energies, particularly photovoltaic (PV), has been attracting increasing attention. Renewable solar energy has become popular due to its potential as an unlimited, non-polluting energy resource. To optimize the use of photovoltaic module arrays, maximum power point tracking (MPPT) is generally used. in conjunction with a power converter. The aim of MPPT is to ensure that the system can always capture the maximum power generated by the solar panels. [2]

In this chapter, we present photovoltaic solar energy and its advantages. We begin with the solar cell, then move on to the photovoltaic system. Next, we explain MPPT control techniques, namely the classical P&O-based method and two intelligent, AI-based techniques: ANN and GA. We also examine the impact of partial shading on the performance of the PV system, a common condition that results in multiple power points and complicates the tracking of the maximum power point.

I.2 Types of renewable energy

Renewable energies come from clean, inexhaustible natural sources such as the solar, wind, tides, rivers, geothermal heat, and biomass. Unlike fossil fuels such as oil, gas, and coal, they represent the future of energy, thanks to their sustainability. Often referred to as “clean energies” or “green energies”, they are perfectly aligned with the energy transition because of their low impact in terms of waste and polluting emissions.[3]



Figure I. 1 : Types of renewable energy.[4]

I.3 Solar energy

Solar energy is the fraction of electromagnetic energy extracted by photosensitive cells from the sun in the form of radiation. figure I.2

Photovoltaic solar energy is one of the most widely used renewable energies, directly converting electromagnetic radiation into electricity through the photovoltaic effect. It has the advantage of being non-polluting, flexible and reliable [1].

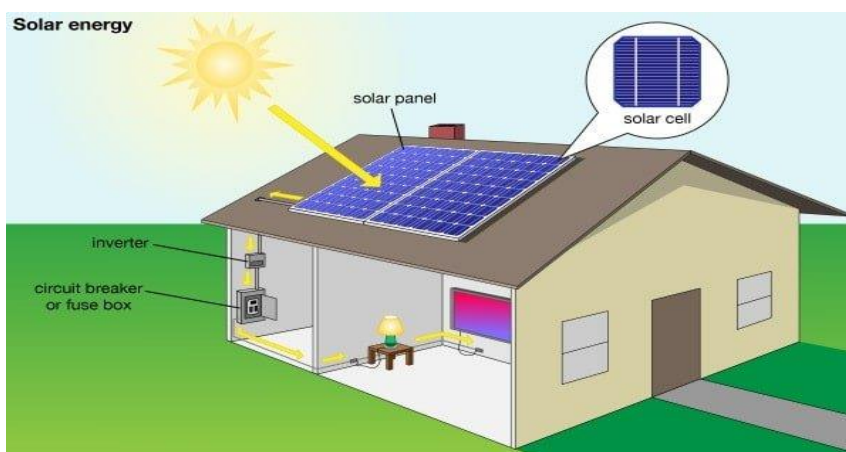


Figure I. 2: Photovoltaic solar energy.[5]

Solar radiation is divided into four parts, figure I.3

- **Global radiation:** This is the solar radiation that reaches ground level on a horizontal surface, either directly or after scattering. It is expressed simply as the sum of scattered radiation.

- **Reflected radiation:** It is reflected by the Earth's surface, either in a preferred direction (specular reflection) or diffusely. The ground reflects radiation in a diffuse and anisotropic manner.
- **Direct radiation:** Direct solar radiation is that which reaches the ground without being scattered. It can be measured using a pyr heliometer.
- **Scattered radiation:** Radiation from the entire celestial vault. This radiation is due to the absorption and scattering of part of the sun's rays by the atmosphere, and their reflection by clouds. It can be measured using a pyranometer with a screen masking the sun.

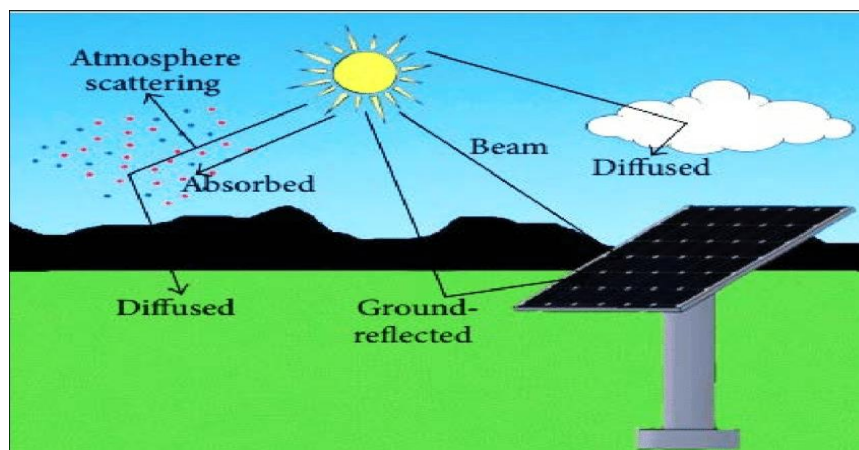


Figure I. 3 : Solar radiation.[6]

I.4 Photovoltaic energy

Photovoltaic energy is based on the photoelectric effect. This creates a direct electric from electromagnetic radiation. The sun emits this type radiation, this resource has the advantage of being inexhaustible and usable at any point territory.

It's also a clean source of energy, since the production of energy from PV modules generates no GHGs (greenhouse gases).

Production is invariably linked to climatic conditions, and a considerable surface area is required to produce large quantities of energy, since the efficiency of PV panels is relatively low (typically between 10 and 18%).[7]

I.4.1 History of photovoltaic energy

The phenomenon was discovered in the 19th century by physicist Alexandre Edmond Becquerel. The first photovoltaic cell was developed in early 1954 for powering satellites. Since 1958, photovoltaic cells have been used exclusively to power satellites, until their first terrestrial applications in the early 1970s. Photovoltaics were used to power small isolated houses and telecommunications equipment.[8]

Some important dates in photovoltaic energy:

1839: French physicist Edmond Becquerel discovered the process of using sunlight to produce electric current in a solid material. This is the photovoltaic effect.

1875: Werner Von Siemens presents a paper on the photovoltaic effect in semiconductors to the Berlin Academy of Sciences.

1912: Albert Einstein was the first to explain the photovoltaic effect, and was awarded the Nobel Prize in Physics in 1921 for this explanation.

1954: Three American researchers, Chapin, Pearson and Prince, develop a high-efficiency photovoltaic cell at a time when the fledgling space industry is looking for new solutions to power its satellites.

1958: A cell with an efficiency of 9% is developed. The first satellites powered by solar cells are sent into space.

1973: The first home powered by photovoltaic cells is built at the University of Delaware.

1983: The first photovoltaic-powered car covers a distance of 4,000 km in Australia.

1995: Grid-connected photovoltaic rooftop programs were launched in Japan and Germany, and have been in widespread use since 2001.

I.5 Photovoltaic cells

A photovoltaic cell is an electronic component which, when exposed to light, generates electricity through the photovoltaic effect. The photovoltaic cell is an elementary electrical generator that converts solar energy directly into electricity.

In a photovoltaic cell, the absorption of photons releases negatively-charged electrons and positively-charged "holes". These are collected by an electrode, creating a potential difference between the two terminals. The photovoltaic cell delivers a DC voltage.[8]

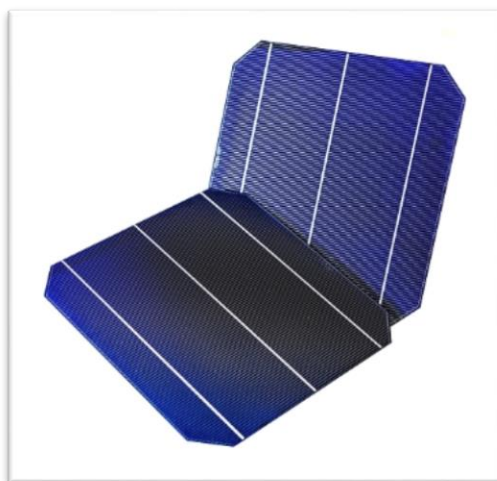


Figure I. 4 : Photovoltaic cells. [9]

I.5.1 Principle of cell operation

Photovoltaic cells are based on the properties of semiconductors which, when struck by photons, set a stream of electrons in motion. Photons are elementary particles that carry solar energy at 300,000 km/s, and which Albert Einstein called “grains of light” in the 1920s. When they strike a semiconductor element like silicon, they strip electrons from its atoms. These electrons set off in a disorderly fashion, looking for other “holes” to reposition themselves in.

But for there to be an electric current, the electrons must all be moving in the same direction. To help them do this, we combine two types of silicon. The side exposed to the sun is “doped” with phosphorus atoms, which have more electrons than silicon, while the other side is doped with boron atoms, which have fewer electrons. This double side becomes a kind of battery: the side with the highest electron content becomes the negative terminal (N), the side with fewer electrons becomes the positive terminal (P). An electric field is created between the two (figure I.5).

When the photons excite the electrons, they migrate to the N zone thanks to the electric field, while the “holes” go to the P zone. They are collected by electrical contacts deposited on the surface of the two zones before going into the external circuit in the form of electrical energy. A direct current is created. An anti-reflective coating prevents too many photons from being lost when reflected by the surface.[1]

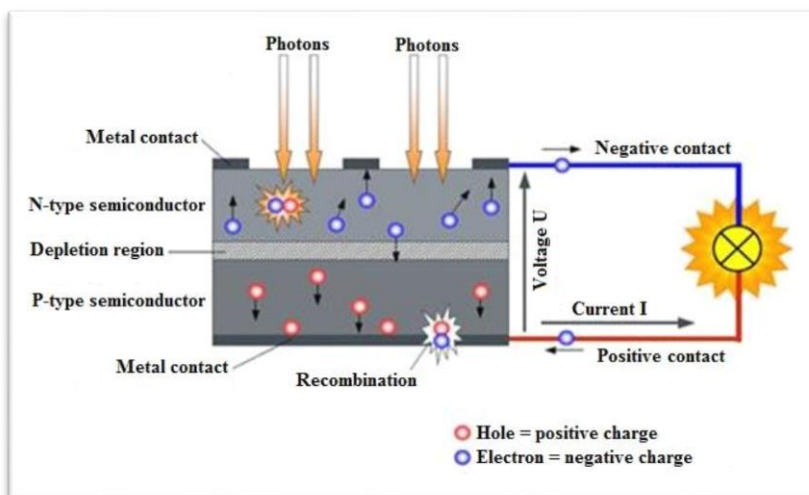


Figure I. 5 : Principle of a photovoltaic cell.[10]

I.6 Advantages and disadvantages of photovoltaic energy

Photovoltaic energy has a number of advantages, but it also has some disadvantages, which are outlined below [7].

I.6.1 Advantages of photovoltaic energy

- Energy from the sun is the most renewable of all sources.
- On isolated sites, photovoltaic energy offers a practical solution for obtaining electricity at lower cost.
- Resale of surplus production helps to amortize investments and even generate income.
- Photovoltaic energy is a clean, non-polluting form of energy that emits no greenhouse gases and generates no waste.

I.6.2 Disadvantages of photovoltaic energy

- The high investment cost of photovoltaic panels.
- The manufacture of photovoltaic panels is a high-tech business, requiring a great deal of research and development, and therefore costly investment. As a result, installation costs are still quite high.
- Photovoltaic panel yields are still low.

- In the case of a stand-alone photovoltaic installation that does not sell its surplus electricity to the grid, batteries must be included, the cost of which remains very high.
- The level of electricity production is not stable and not predictable, but depends on the level of sunlight. In addition, there is no electricity production in the evening and at night.

I.7 DC-DC converters

DC-DC converters are electronic devices that convert one DC voltage into another variable DC voltage. In general, DC-DC converters are used to improve energy efficiency, reduce power losses and regulate supply voltage more precisely in electronic systems. There are several types of DC-DC converters, each with its own characteristics and advantages. The most common are BUCK, BOOST and BUCK-BOOST converters. [11]

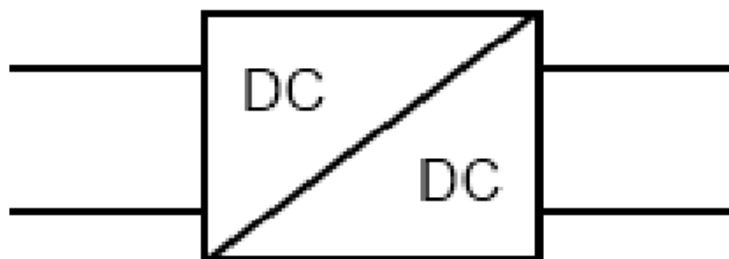


Figure I. 6 : Symbol of DC-DC converter. [12]

I.8 Types of DC-DC converters used in photovoltaic systems

DC-DC converters (or choppers) are used in solar energy systems to adapt the variable-amplitude DC source (PV panel) to the load, which generally requires a constant DC voltage. The three basic configurations are: [11]

- buck converter
- Boost converter
- Buck-to-boost converter

In our study, we're interested in the boost converter.

I.9 The MPPT control

The MPPT is essential in the operation of the PV arrays to improve the overall system efficiency. The solar irradiation (G) and the cell temperature (T) are considered to represent the environmental conditions change along the day hours. As G and T vary, the PV array voltage and power depart from the optimum point. Consequently, the PV array voltage is adjusted to match the maximum output power. The common way to adjust the PV voltage is via adjusting the duty cycle of the DC-DC boost converter. The most widespread MPPT the perturb-and-observe. Driven by the advancements in artificial intelligence techniques. Many variants are applied as a control methods to the PV system . For PV modules, there is one single operating point from where maximum power can be drawn. This point is required to be located or tracked and we need to make sure that functional position of PV module is always at or around this maximum power point. The various MPPT techniques are being established and realized. These techniques differ over-complication, required sensors, implementation charges, tracking time, effective operating range, hardware implementation, acceptance, and reverences. The coming sections present the assessment of several MPPT techniques available and their relative advantages and disadvantages.[8]

I.10 Classification of MPPT controllers

The literature proposes several MPPT algorithms that can be divided into two main categories: conventional and unconventional.[3]

I.10.1 Conventional methods

Conventional methods are divided into two types:

- **Indirect methods**

In indirect methods, databases containing the physical values of the PV panel are generally used to generate control signals under different climatic conditions (temperature, irradiance). These methods, used only for PV systems, are the open-circuit voltage method (V_{oc}) and the short-circuit current method (I_{sc}).

- **Direct methods**

Instantaneous values of PV output voltage or current are generally used to generate the control signals, and the algorithm is based on the variation of these measurements. The advantage of these algorithms is that they do not require prior knowledge of PV panel characteristics. It can therefore

react to unpredictable changes in PV operation. To achieve this, the operating point voltage is incremented at regular intervals. If the output power is higher, then the search direction is maintained for the next step; otherwise, it is reversed.

Like incremental conductance (Inc.C), escalation (HC) and the most widely used, perturb and observe (P&O). Escalation (HC) is based on disturbance of the duty cycle of the connected power converter. Incremental conductance (Inc.C) is calculated using the PV system's power derivative, respecting its voltage, which must be equal to zero at MPP; however, it would be positive to the left of MPP and negative to the right. The P&O, generally similar in concept to the HC method, is an iterative technique for MPPT; it measures photovoltaic characteristics and then disturbs the respective operating point of the PV system to respond to the direction of change.

I.10.2 Non-conventional (intelligent) methods

In recent years, more robust control techniques have been associated with MPPT control, such as fuzzy logic, neural networks and neuro-fuzzy systems.

In general, all AI-based MPPT techniques feature fast convergence speed, fewer steady-state oscillations, and high efficiency compared to conventional MPPT techniques. However, AI-based MPPT techniques are computationally intensive and costly to implement.

In our work, we have presented some methods (conventional and non-conventional) for monitoring the operating point at maximum power of the photovoltaic system, which are:

- P&O method.
- ANN method.
- GAs method .

I.11 The perturb and observe (P&O) method

This is the most commonly used method. It is an iterative method for obtaining the maximum power point (MPP). The principle of this method is based on varying the generator voltage V_{pv} around its initial value by acting on the duty cycle D while observing the behavior of this variation on the power P_{pv} . According to the resulting change, if the positive overvoltage of the V_{pv} voltage generates an increase in the P_{pv} power, it means that the operating point is to the left of MPP. [1]

If power decreases, the operating point has exceeded MPP. Similar reasoning can be applied when voltage decreases by reversing the direction of variation of the duty cycle D (figure I.6).[1]

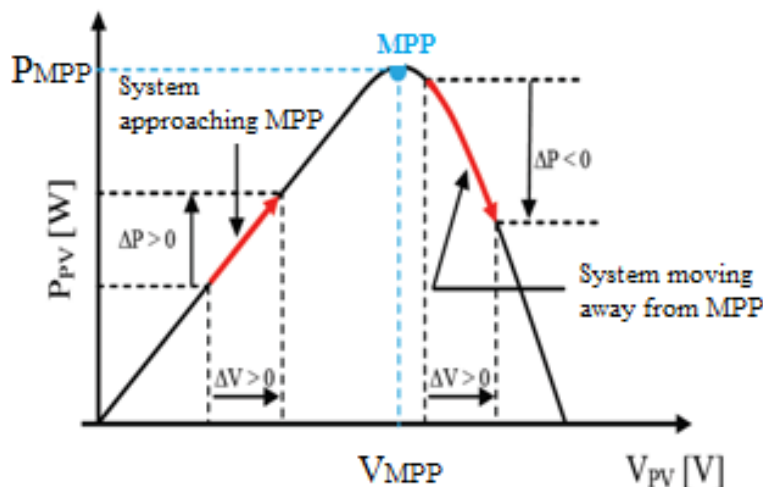


Figure I. 7 : Characteristic P_{pv} (V_{pv}) P&O.[13]

I.12 Artificial neural networks

Neural networks, made up of artificial cellular structures, offer a new approach to the problems of perception, memory, learning and reasoning. They are also proving to be a highly promising alternative to some of the limitations of conventional computers. Thanks to their parallel processing of information and their mechanisms inspired by nerve cells (neurons), they infer emergent properties that enable the solution of complex problems.[14]

I.12.1 History

In 1948, American researchers Mac Culloch and Pitts created the first mathematical model of a biological neuron, called a "formal neuron." This binary neuron knows only 0 or 1 responses.

In 1949, Canadian psychologist Donald Hebb proposed Hebb's famous law to explain the learning, memory, and conditioning effects of cells as a function of their simultaneous activity. At the same time.

In 1951, Minsky created the first real model of a neural network, called a "neural computer" or Smarl.

In 1957, Rosenblatt developed the perceptron model, the first neurocomputer applied to pattern recognition.

In 1960, Widrow developed the Adaline model, similar to the perceptron but with a different learning law, the origin of the gradient back-propagation algorithm.

In 1969, Minsky and Papert published a book highlighting the theoretical limitations of the perceptron and, implicitly, of all artificial neural network models. In the 1970s, researchers and investors turned their attention away from neural networks and towards the symbolic approach to artificial intelligence. However, in 1982, Hopfield demonstrated the analogy of neural networks with certain physical systems, enabling the application of a rich and masterful formalism.

In 1985, new mathematical models made it possible to overcome the limits of the perceptron. Since then, neural networks have become a highly effective tool for system control and modeling, signal and image processing, thanks to their classification, memorization, filtering and approximation capabilities.[14]

I.12.2 Biological foundation

The brain is made up of around 10^{12} interconnected neurons, with 1000 to 10000 synapses per neuron. Not all neurons are identical, nor do they behave in the same way. In our work, we focus on the fundamental principles required to understand how neural networks work.[15]

I.12.2.1 Biological basis

A neuron is a particularly complex cell specialized in the processing of electrical signals. Its role is to receive, store and transmit information (figure I.7).

The neuron can be broken down into three main regions: the cell body, the dendrites and the axon.[15]

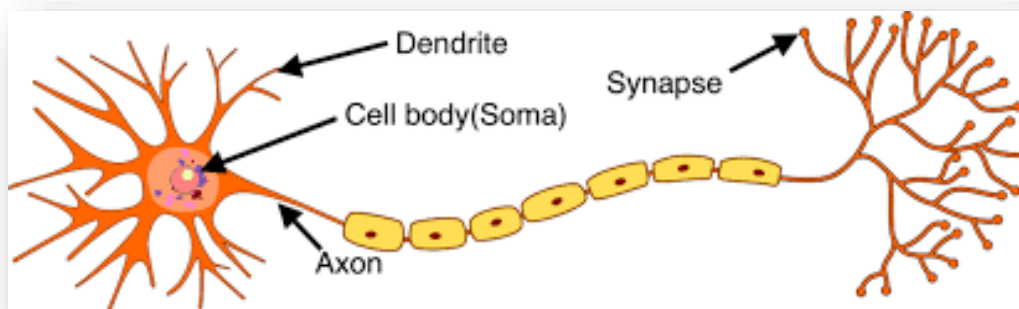


Figure I. 8: Biological neuron.[16]

The Constitution of the biological neuron are shown in following table I.1

Table I. 1: Function of the biological neuron.[17]

Part	Function
Cell body	Receiving the nerve flow Treatment Activation
Axons	Transmission
Synapses	Electrical-chemical transformation Transmission du signal provenant de l'axone Receiving the chemical electrical signal
Dendrites	Routing signals from other cell bodies 0

I.12.3 mathematical model (artificial neuron)

The mathematical model of an artificial neuron is illustrated in figure (III.2). A neuron essentially consists of an integrator that performs a weighted sum of its inputs. The result V of this sum is then transformed by a transfer function Q which produces the neuron's output Y . The neuron's m inputs correspond to the vector $x = [x_1, x_2, \dots, x_m]$, while $W = [W_1 \dots W_m]$ represents the neuron's vector of weights. The integrator's output V is given by the following equation:[15]

$$V = \sum_{j=1}^m w_j \cdot x_j - b \quad (\text{III.1})$$

$$= W_1 \cdot x_1 + W_2 \cdot x_2 + \dots + W_m \cdot x_m - b \quad (\text{III.2})$$

$$Y = Q(V) = Q\left(\sum_{j=1}^m W_j \cdot x_j - b\right) \quad (\text{III.3})$$

which can also be written in matrix form:

$$V = W^T \cdot x - b \quad (\text{III.4})$$

$$y = Q(V) = Q(W^T \cdot x - b) \quad (\text{III.5})$$

$$W = \begin{bmatrix} W_1 & \cdots & W_{1,m} \\ \vdots & \ddots & \vdots \\ W_S & \cdots & W_{S,m} \end{bmatrix} \quad x = [x_1, x_2 \dots x_m] \quad (\text{III.6})$$

This output corresponds to a weighted sum of weights and inputs, minus what we call the neuron's b-bias. The result v of the weighted sum is called the neuron's activation level. The bias b is also called the neuron's activation threshold. When the activation level reaches or exceeds the threshold b , the argument of Q becomes positive (or zero). Otherwise, it becomes negative.

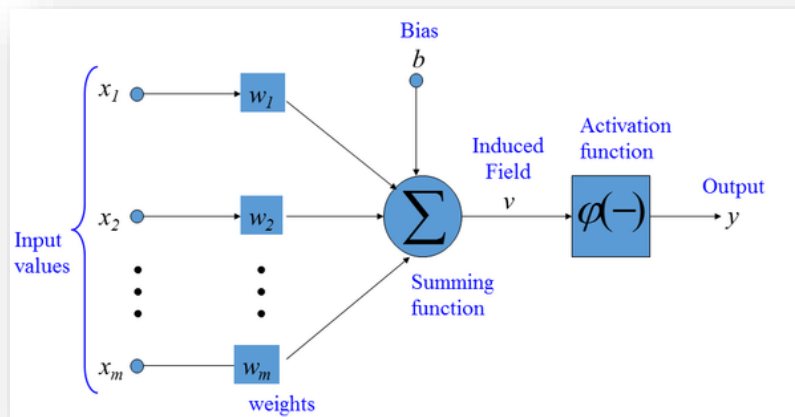


Figure I. 9: Artificial neuron model [18]

I.12.3.1 Activation Function

By computing the weighted sum and then applying bias, the activation function determines if a neuron needs to be stimulated or not. Adding non-linearity to a neuron's output is the aim of the activation function. We are aware that each neuron in the neural network responds to weight, bias, and its corresponding activation function. Based on the mistake in the output, we would adjust the weights and biases of the neurons in a neural network. We call this method back-propagation. Back-propagation is made possible by activation functions, which provide the gradients and error together for updating the weights and biases .[19]

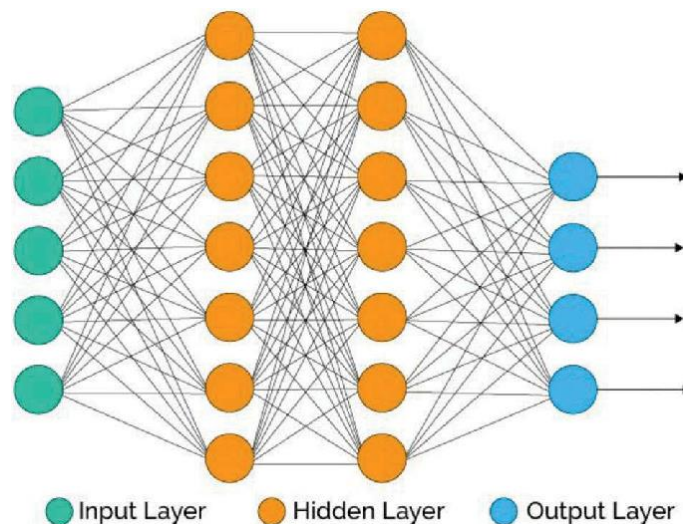
Table I. 2: Activation functions [15]

Function	formula
threshold	$f(x) = \begin{cases} 0 & \text{si } x < 0 \\ 1 & \text{si } x \geq 0 \end{cases}$
Symmetrical threshold	$f(x) = \begin{cases} -1 & \text{si } x < 0 \\ 1 & \text{si } x \geq 0 \end{cases}$
Linear	$f(x) = X$
Sigmoid	$f(x) = \frac{1}{1 + e^{-x}}$
Hyperbolic tangent	$f(x) = \frac{1 - e^{-x}}{1 + e^{-x}}$

I.12.4 Neural Network Architecture

I.12.4.1 Non-looped networks

The output signal is obtained directly after application of the input signal. They are unidirectional with no feedforward, and have the structure of a combinatorial system.[17]

**Figure I. 10:** Non-looped networks.[20]

- **Input layer:** this layer receives the raw data fed into the network.

- **Hidden layers:** The performance of these layers is determined by the inputs and weights of the connection between them and the hidden layers. The weights between the input and hidden neurons determine when a neuron in that layer should be activated.
- **output layer :** The output of the output unit depends on the activity of the hidden layer and the weights of the connection between the hidden unit and the output.[21]

I.12.4.2 Looped networks

With feedback (feedback network or recurrent network), they have a structure similar to that of sequential systems.[17]

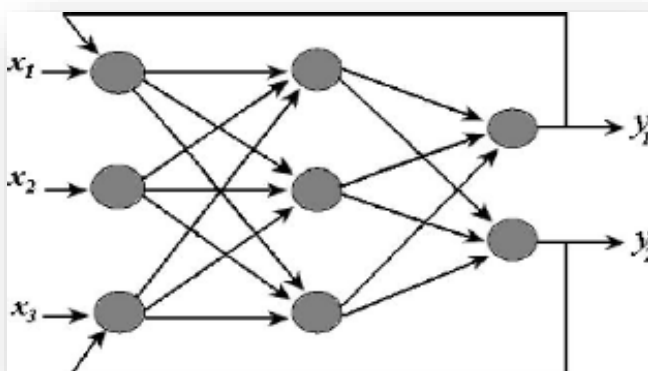


Figure I. 11: Looped networks.[22]

I.13 Genetic Algorithms

Genetic algorithms are optimization algorithms based on techniques derived from genetics and evolutionary mechanisms in nature: selections, crossovers, mutations, etc. They belong to the class of evolutionary algorithms. Genetic algorithms can be said to be programming methods based on the principle of evolution, in the search for a suitable solution to a problem.[23]

I.13.1 Basic definitions of genetic algorithms

Some definitions of the constituents of the genetic algorithms adopted for composite materials are given [24]:

Population: a set of individuals, randomly generated according to chromosome number.

Individual: is a member of the population who carries several chromosomes.

Chromosome: a set of variables for the individual.

Gene: is a basic chromosome segment. It characterizes the value of a variable in the solution to the problem addressed by the genetic algorithm.

Locus: the position of the gene on the chromosome.

Allele: a symbol for coding a gene. In natural genetics, four letters ATCG are used, or a binary alphabet 1 or 0 is generally used.

Mutation: random change of an allele during the reproductive phase.

Crossover: positional exchange between alleles of two genes from two different individuals.

Reproduction: duplication by crossing and mutation of chromosomes to give rise to new individuals.

Objective function: function quantifying the performance of a target objective: minimum mass, maximum resistance...

Adaptation function or performance function: function combining several objective functions and quantifying an individual's performance with a numerical value.

I.13.2 History and principle

Genetic algorithms were developed by John Holland in the 1970s at the University of Michigan. In 1975, Holland introduced the first formal genetic algorithm. It explains how to evolve a computer program through crossover and mutation. Thanks to the book written by D. E. Goldberg in 1989, GAs became known in the scientific community, and we owe their popularization to the release of powerful calculators in the 90s, marking the beginning of a new interest in this optimization technique.[25]

The GA principle is simple, and comprises three phases:

- 1 - Genesis (the random initialization of individuals to form the population of the first generation)
- 2 - Reproduction (the evolution of individuals from the current generation to the next) :

-selection of reproductive individuals.

-genetic cross-breeding of these individuals to create new individuals.

-mutation of certain individuals so that genetic creation does not weaken.

-evaluation of individuals by calculating their adaptation function.

- 3 - Search for the most suitable individual according to the desired criteria. The solution will be represented by the best individual of the last generation.[25]

I.13.3 The coding

Coding is the modeling of a solution to a given problem in the form of a sequence of characters called a chromosome, which is a set of genes representing a variable or part of the problem. The main task is to choose the gene content that facilitates the description of the problem and respects its constraints. In the context of GAs, we will present two of the coding representations [26]:

- **Binary coding:** binary coding consists in representing each individual as a string of bits, where each element takes the value 0 or 1. The parameter values are the phenotype's and then supplied to the adaptation function, which returns the performance, enabling the individual to be classified in the population.
- **Real coding:** for certain continuous optimization problems, real coding offers better performance than binary coding. Chromosomes are represented as a vector $(x_1, x_2, x_3 \dots x_n)$ where each x_i is a real number (the gene) that represents a variable in the problem. The possible values of the genes are contained within the interval defined by the variables they represent, and genetic operators must take this constraint into account.

I.13.4 Generation of the initial population

This step consists of selecting a set of potential solutions to the given optimization problem. Each individual, or chromosome in Holland's (1975) terminology, is represented by a potential solution. All these individuals are then brought together in what is known as the initial population.[26]

I.13.4.1 Evaluation (fitness)

The evaluation function, or fitness, consists in measuring the performance of each individual in the population. Evaluation ensures that the best-performing individuals are retained so that they can be selected (selection operator) and then modified (crossing and mutation). Unsuitable individuals, on the other hand, are gradually eliminated from the population. The complexity of the evaluation function depends essentially on the problem and its constraints.[26]

I.13.4.2 Genetic Operations

Genetic operations are the base of GAs; they do not exclude probability theories, but they give very interesting results. These operations are [27]:

1. **Selection:** Select, with a rate T_{sel} (%), a part of the population corresponding to the optimum fitness; in nature, only the individuals more adapted to the environment will survive. The roulette wheel selection method is used.

2. **Crossover:** After selection, natural reproduction is performed by crossing pairs of individuals.



3. **Mutation:** After crossover, we apply a mutation, with small probability P_m (for example: the probability of parents with blue eyes to have a child with brown eyes).



4. **Insertion:** The new population will be integrated to the old one to replace individuals with the minimum fitness function, so a new generation contains the same number of individuals.
5. **Program Termination :** The program creates new optimal individuals. It ends after a set number of iterations, so we obtain a constant execution time. Many tests were performed to choose an iteration number that balances optimal results and processing time.

I.14 Partial shading

Partial shading concerns half a cell or half a row of cells. This effect will reduce power in proportion to the percentage of the surface shaded.

When PV cells are linked in series, the current flowing through the array is limited by the cell with the lowest performance or the least light. This means that a cell that does not receive the same amount of light as the rest of the array will produce a lower current; this is known as partial

shading. Because of partial shading, the cell receiving the least flux will dissipate some of the energy produced by the rest. The whole would produce a weaker current; this is known as partial shading.[28]



Figure I. 12 : Partial shading of photovoltaic panels . [29]

I.14.1 Causes of shading

Many factors can cause partial shading, such as trees, clouds, snow, sand, dust, power poles and buildings.[28]

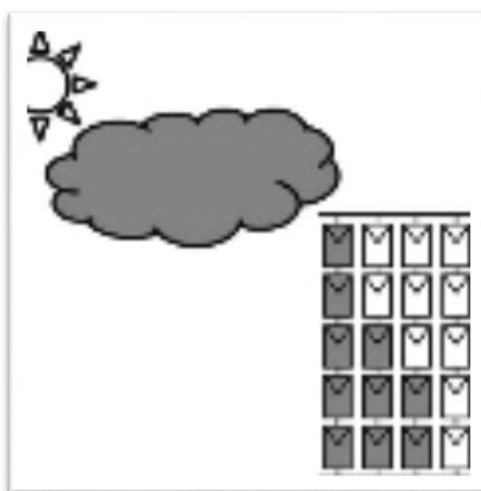


Figure I. 13 : PV system under partially shaded conditions caused by passing clouds.[30]

I.14.2 The partial shading effect

The partial shading effect is related to the power losses of a solar cell, module, or array operating under different weather conditions. These include soiling, poorly soldered cells, non-uniform irradiation, temperature variations, and cell cracking. The partial shading effect regroups all

conditions that lead to a change in the photocurrent of the PV module/array. These conditions reduce current production of the cell or module. Thus, the modules, operating normally impose their higher current over any shaded PV module connected in series, forcing these into reverse bias and dissipating power. In addition, when the shaded PV module's temperature exceeds a critical value, allowed of PV cells in the PV module, cracking may occur. This phenomenon is called Hot Spot.[31]

I.14.3 By-pass diode for a photovoltaic solar module

The bypass diode is connected antiparallel to a group of cells to protect the weakest cells from reverse bias; this diode will be conductive. In the case of shading of one or more cells in a branch, and blocked in the normal case, and enabling the entire string not to be lost (by-pass diode) and hot spots to be avoided. [2]

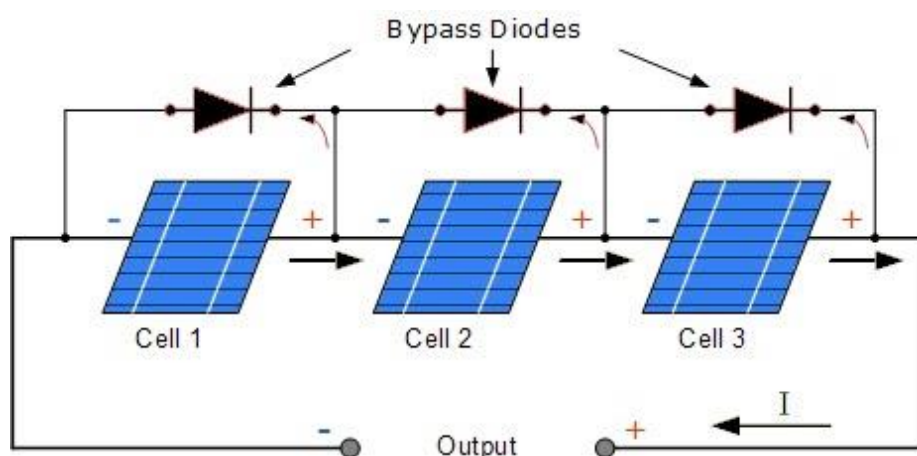


Figure I. 14 : Use of the by-pass diode.[32]

I.15 Conclusion

In this chapter, we have presented a general overview of photovoltaic systems, starting with solar energy and the photovoltaic effect, then explaining how the photovoltaic cell works and the advantages and disadvantages of a PV system. We also covered DC-DC converters and MPPT control, detailing the main algorithms used for maximum power point tracking, namely: P&O, ANN and GA. In addition, we studied the phenomenon of partial shading, its causes and its impact on photovoltaic panel performance.

In the next chapter, we introduce the modeling of the photovoltaic system and the boost converter. We then study MPPT control using the P&O method, followed by a simulation in MATLAB/SimpowerSystems, with an analysis and discussion of the results obtained.

Chapter II

***Dynamic Simulation and Optimization of PV
Systems with MPPT Control***

II.1 Introduction

To optimize a photovoltaic generator and make the best possible use of the energy extracted, we need to adapt the non-linear current-voltage characteristic of the photovoltaic generator to the operating point of the load used. To find the optimum point, which corresponds to the point of maximum power, it is obvious to model the photovoltaic generator.[33]

In this chapter, we present the modeling of a photovoltaic module. We analyze the operation of a boost converter. We finalize the analysis of the P&O based MPPT technique. The software used to simulate the system is the MATLAB/Simpower system.

II.2 Modeling of a photovoltaic cell

The PV cell is the basic element of PV generator, which converts solar irradiation into electrical energy. The most widely used model for its simplicity and accuracy is that of a diode, which is illustrated in Figure II.1.

A cell series resistance R_s is attached in series with a parallel combination of cell photocurrent I_{ph} , exponential diode, and shunt resistance R_{sh} . [34]

I_{pv} , and V_{pv} are the PV cell's current and voltage respectively.

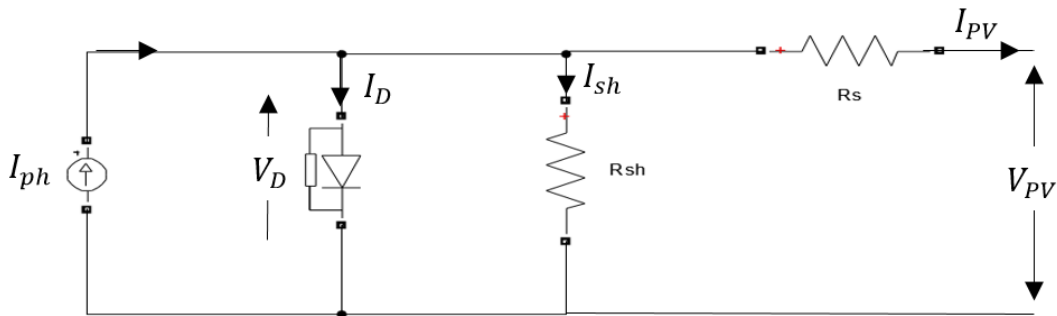


Figure II. 1 : Equivalent model of the PV cell.

Kirchhoff's law applied to the above circuit, gives:

The output current of the PV array:

$$I_{pv} = I_{ph} - I_d - I_{sh} \quad (\text{II.1})$$

With:

- Photocurrent:

$$I_{ph} = (I_{sc} + K_i(T-T_n)) * \left(\frac{G}{G_n}\right) * N_{pp} \quad (\text{II.2})$$

- Current flowing through the diode:

$$I_d = I_s \left(\exp\left(\frac{V_{pv} + I_{pv} * R_s}{v_t}\right) - 1 \right) \quad (\text{II.3})$$

- Thermal voltage:

$$V_t = N_{ss} * \frac{k(T+273.15)}{q} \quad (\text{II.4})$$

- Saturation current:

$$I_s = I_{rs} * N_{pp} * \left(\frac{T+273.15}{T_n+273.15}\right)^3 * \exp\left(\frac{q * E_g}{n * k} \left(\frac{1}{T_n+273.15} - \frac{1}{T+273.15}\right)\right) \quad (\text{II.5})$$

- Current flowing through the shunt resistor R_{sh} :

$$I_{sh} = \frac{V_{pv} + I_{pv} * R_s}{R_{sh}} \quad (\text{II.6})$$

According to (II.3) and (II.6), equation (II.1) can be written as follows:

$$I_{pv} = I_{ph} - I_s \left(\exp\left(\frac{V_{pv} + I_{pv} * R_s}{V_t * n}\right) - 1 \right) - \left(\frac{V_{pv} + I_{pv} * R_s}{R_{sh}}\right) \quad (\text{II.7})$$

This equation (II.7) can be extended to PV modules by adding integrating factors for series and parallel cells. As we can see in the figure II.8, the final formula takes into account the total number of series (N_{ss}) and parallel (N_{pp}) cells specified in the source and determines the output current of the PV module relative to its voltage.

$$I_{pv} = N_{pp} \left[I_{sc} \left(1 - \exp\left(\frac{\frac{V_{pv}}{N_{ss}} V_{oc} + R_s \frac{I_{pv}}{N_{pp}}}{n * V_t}\right) \right) \right] \quad (\text{II.8})$$

II.2.1 Presentation and simulation of the PV module:

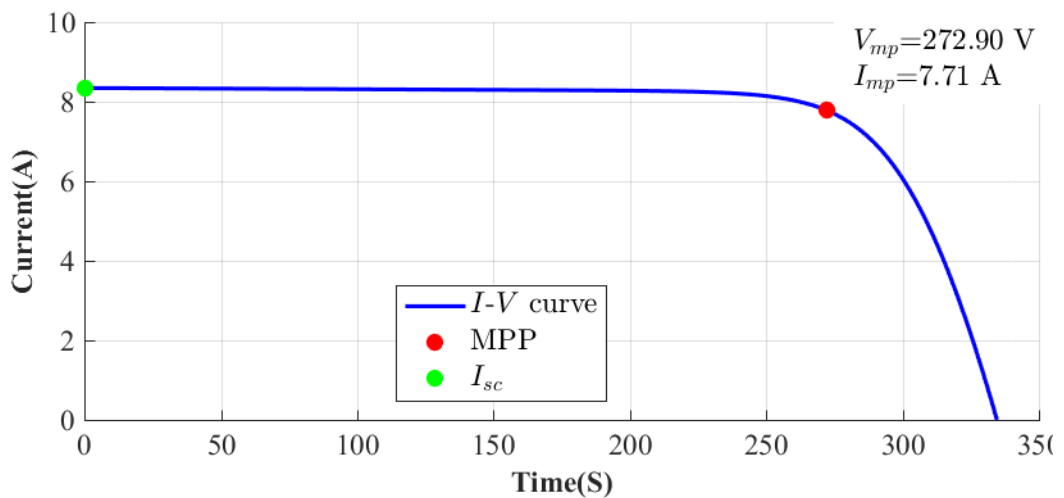
The electrical characteristics are shown in the following table II.1

Table II. 1: Electrical characteristics of the photovoltaic panel.

Dimensions	values
Maximum power, P_{max}	235.2672 W
Voltage at P_{max} , V_{mp}	30.24 V
Current at P_{max} , I_{mp}	7.78 A
Open circuit voltage, V_{oc}	37.2 V
Short-circuit current, I_{sc}	8.35 A
Number of cells in series, N_{ss}	9
Number of cells in parallel, N_{pp}	1
Series resistance, R_s	0.25 Ω
Shunt resistance, R_{sh}	350 Ω

In order to get 2100W (specifically in our work) or any other power, we preferred to use the mathematical modeling of the PV array with the help of the equations above. The current-voltage (I-V) and the power-voltage (P-V) characteristics of the photovoltaic system were simulated using MATLAB/SimPower System under standard test conditions ($T = 25^\circ\text{C}$ and $G = 1000 \text{ W/m}^2$).

The resulting curves are presented in the following figures II.2 and figure II.3.

**Figure II. 2:** I-V characteristics of PV under standard conditions.

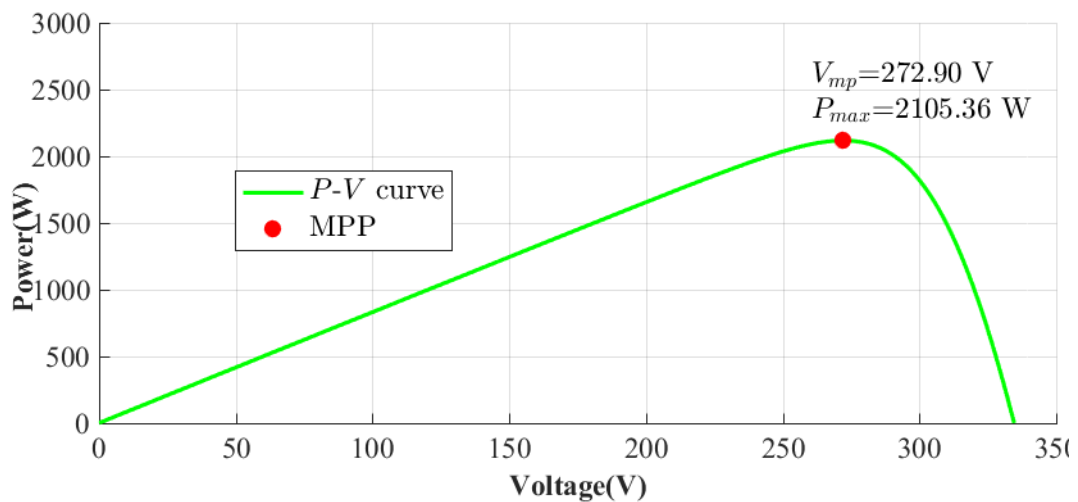


Figure II. 3: P-V characteristics of PV under standard conditions.

II.2.2 Influence of temperature on the PV cell

The two figures below (II.4 and II.5) illustrate the behavior of a solar panel when exposed to an irradiance of 1000 W/m^2 and temperatures ranging from 15°C to 35°C .

From figure II.4, we can see that the effect of increasing temperature reduces the PV open-circuit voltage, while the short-circuit current increase slightly.

According to figure II.5, the power will slowly rise as the temperature increases.

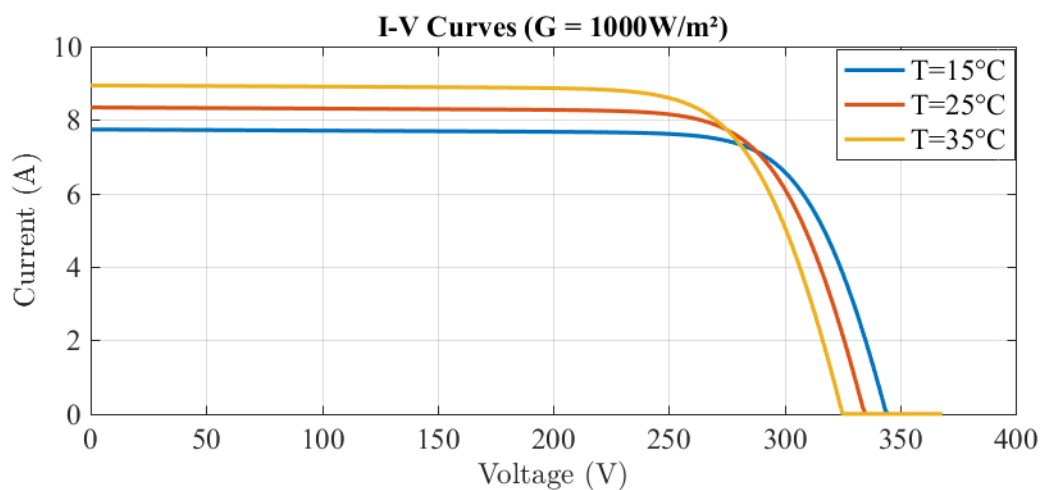


Figure II. 4: Influence of temperature On the I_V characteristics.

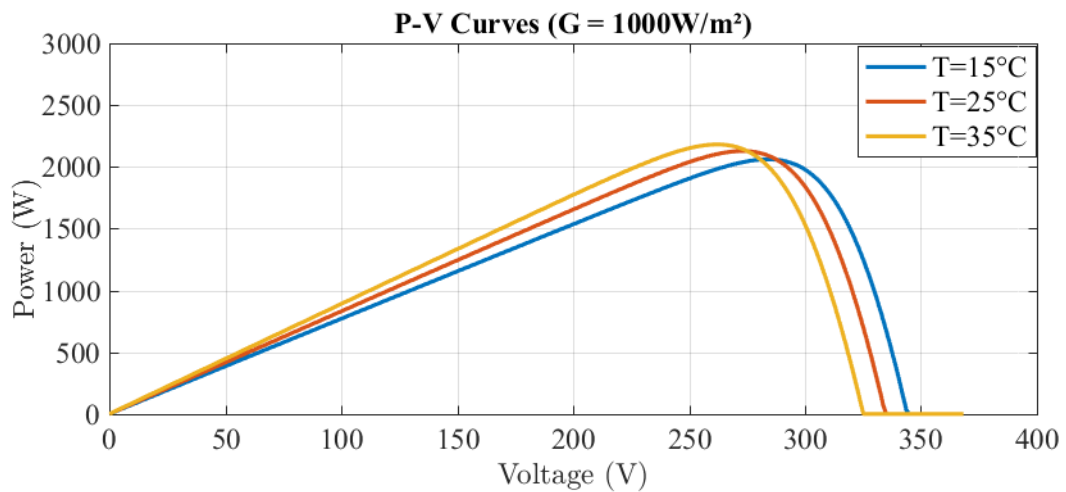


Figure II. 5: Influence of temperature On the P_V characteristics.

II.2.3 Influence of irradiance on the PV cell

The two figures (II.16 and II.17) show the behavior of a photovoltaic panel at a constant temperature of 25°C for different irradiances from 250 to 1000 W/m^2 .

The results show that when the irradiance increases, the power and current of solar photovoltaic increase. In addition, the open circuit voltage increases with increasing solar irradiance.

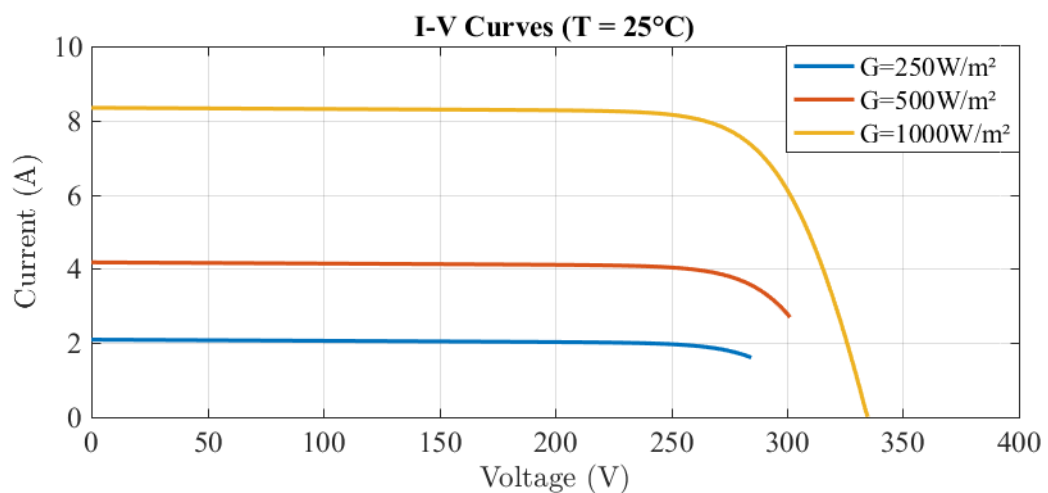


Figure II. 6: Influence of irradiance on The I_V characteristics.

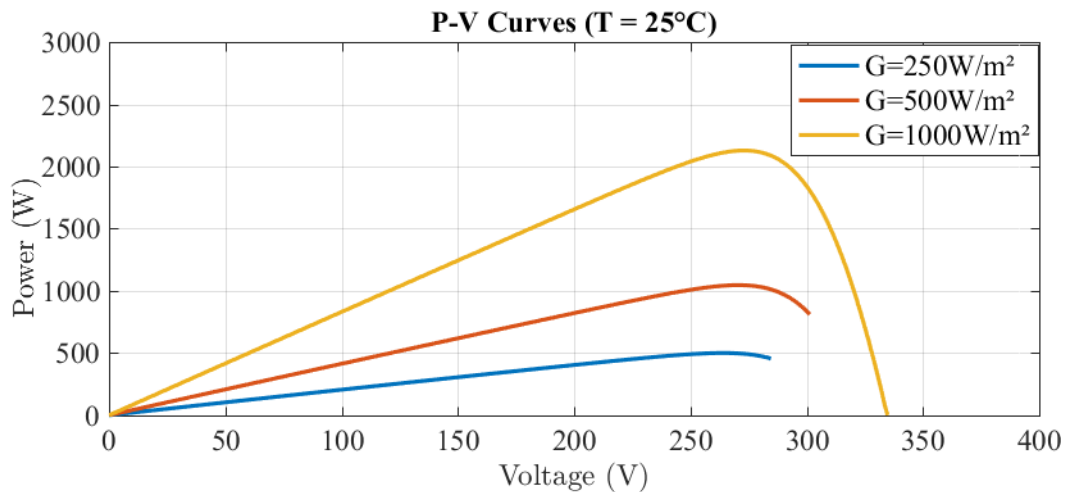


Figure II. 7: Influence of irradiance on The P_V characteristics.

II.3 Modeling of a DC-DC Boost converter

The method of adapting the PV generator to the load is very important to obtain maximum energy as well as high efficiency from the PV module. This is accomplished by used DC-DC power converters, and controlled by the MPPT controller. The control strategy, which causes the voltage change simply lies in adjust the duty cycle appropriately.

In this study, the DC-DC Boost converter was used, which increases the amount of input voltage to the desired output voltage. The boost converter topology is shown in Figure II.8.[34]

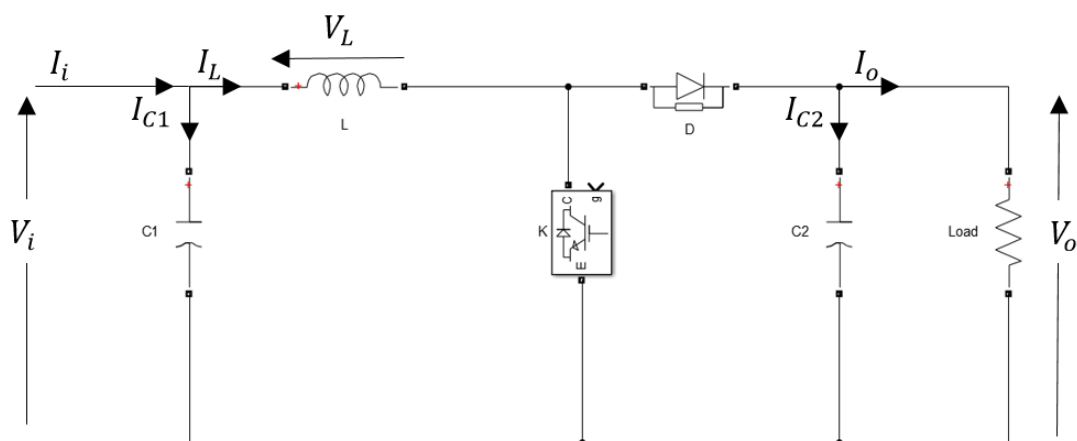


Figure II. 8: Topology of a DC-DC Boost converter.

The electrical characteristics are shown in the following table II.2

Table II. 2: Electrical characteristics of the DC-DC Boost converter.

Parameters	values
Input Voltage, V_i	273.14V
Output Voltage, V_o	600V
Capacitor at the input, C_i	5.7 e-05F
Capacitor at the output, C_o	6 e-06 F
Inductance, L	0.1955H
Frequency of switching, F_{sw}	5000Hz
Resistive Load, R_o	172.7506 Ω

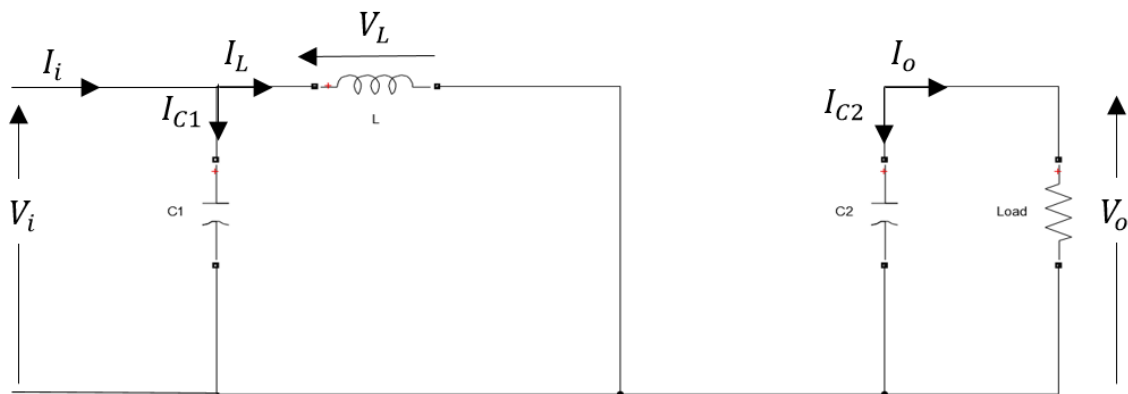
II.3.1 Operation

When the switch is closed for the duration, the current in the inductance increases linearly. The voltage across K is zero. During this time, the switch opens and the energy stored in the inductor drives the current flow in the freewheeling diode. Assuming that the voltage across the inductor is zero, we arrive at [35]

$$V_i = V_o (1 - D) \quad (\text{II.9})$$

II.3.2 Equivalent mathematical model

In order to synthesize the functions of the boost converter at steady state, it is necessary to present the equivalent circuit diagrams at each position of the K switch. Figure II.9 shows the equivalent boost circuit when K is closed.[35]

**Figure II. 9:** Electrical diagram of a closed boost converter.

When Kirchhoff's law is applied to the equivalent circuits of the two operating phases, the following calculations are obtained:

$$I_{C_1}(t) = C_1 \frac{dV_i(t)}{dt} = I_i(t) - I_L(t) \quad (\text{II.10})$$

$$I_{C_2}(t) = C_2 \frac{dV_o(t)}{dt} = -I_o(t) \quad (\text{II.11})$$

$$V_L(t) = L \frac{dI_L(t)}{dt} = V_i(t) \quad (\text{II.12})$$

In the open state of switch K, the circuit equivalent to boost operation is as follows [35]:

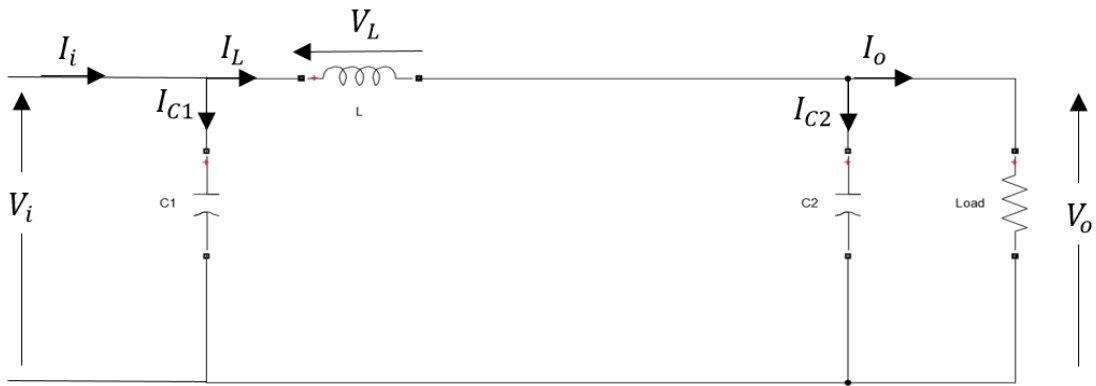


Figure II. 10: Electrical diagram of an open boost converter.

The calculations obtained are:

$$I_{C_1}(t) = C_1 \frac{dV_i(t)}{dt} = I_i(t) - I_L(t) \quad (\text{II.13})$$

$$I_{C_2}(t) = C_2 \frac{dV_o(t)}{dt} = I_L(t) - I_o(t) \quad (\text{II.14})$$

$$V_L(t) = L \frac{dI_L(t)}{dt} = V_i(t) - V_o(t) \quad (\text{II.15})$$

II. 4 MPPT control

An MPPT is a principle for tracking the maximum power point of a non-linear electrical generator. MPPT systems are generally associated with photovoltaic or wind generators. [35]

II.4.1 MPPT principle

MPPT is an essential control that ensures the photovoltaic module operates at its optimum operating point, whatever the load and atmospheric conditions (temperature and irradiance).

The control principle is based on varying the operating point by modifying the duty cycle. To reach the optimum value. [36]

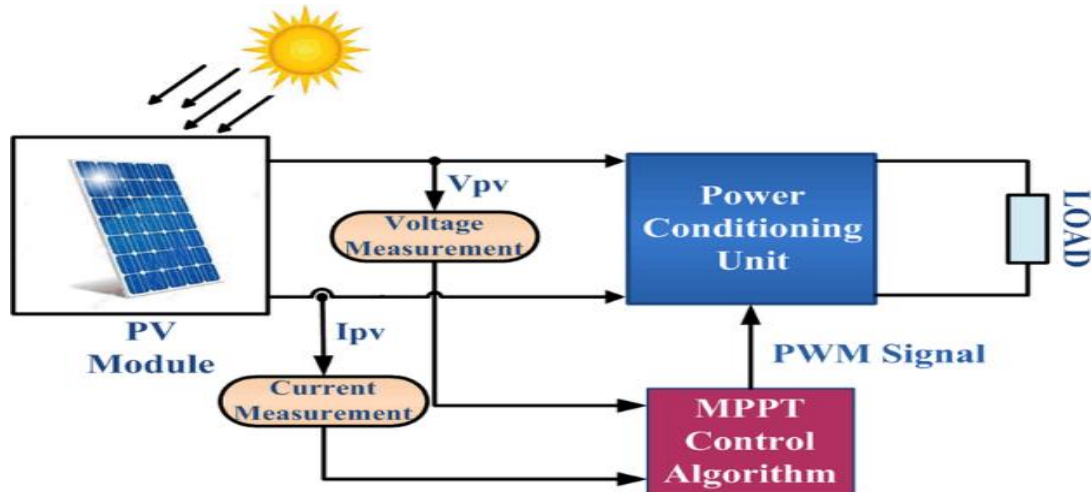


Figure II. 11: Solar energy conversion chain with MPPT control. [37]

When temperature and/or irradiance fluctuate, the MPPT algorithm must also track the new, modified maximum power point in its corresponding curve. As mentioned above, many MPPT algorithms are used in PV systems to track the MPP and produce the maximum available power from the PV array. The P&O method is widely used due to its ease of implementation and simplicity.

II.4.2 Perturb & Observe (P&O) Method

This is the most widely used MPP tracking algorithm, and as its name suggests, it is based on perturbing the system by increasing or decreasing the reference voltage or by acting directly on the converter duty cycle (DC-DC), then observing the effect on output power with a view to a possible correction of this duty cycle (D). [35]

From Figure II.12, it can be seen that when the power increases, the perturbation should remain in the same direction, but when the power decreases, the perturbation should remain in the inverse direction. Based on these findings, we implemented the algorithm. The process is repeated until the MPP is reached. Then, the operating point oscillates around the MPP.

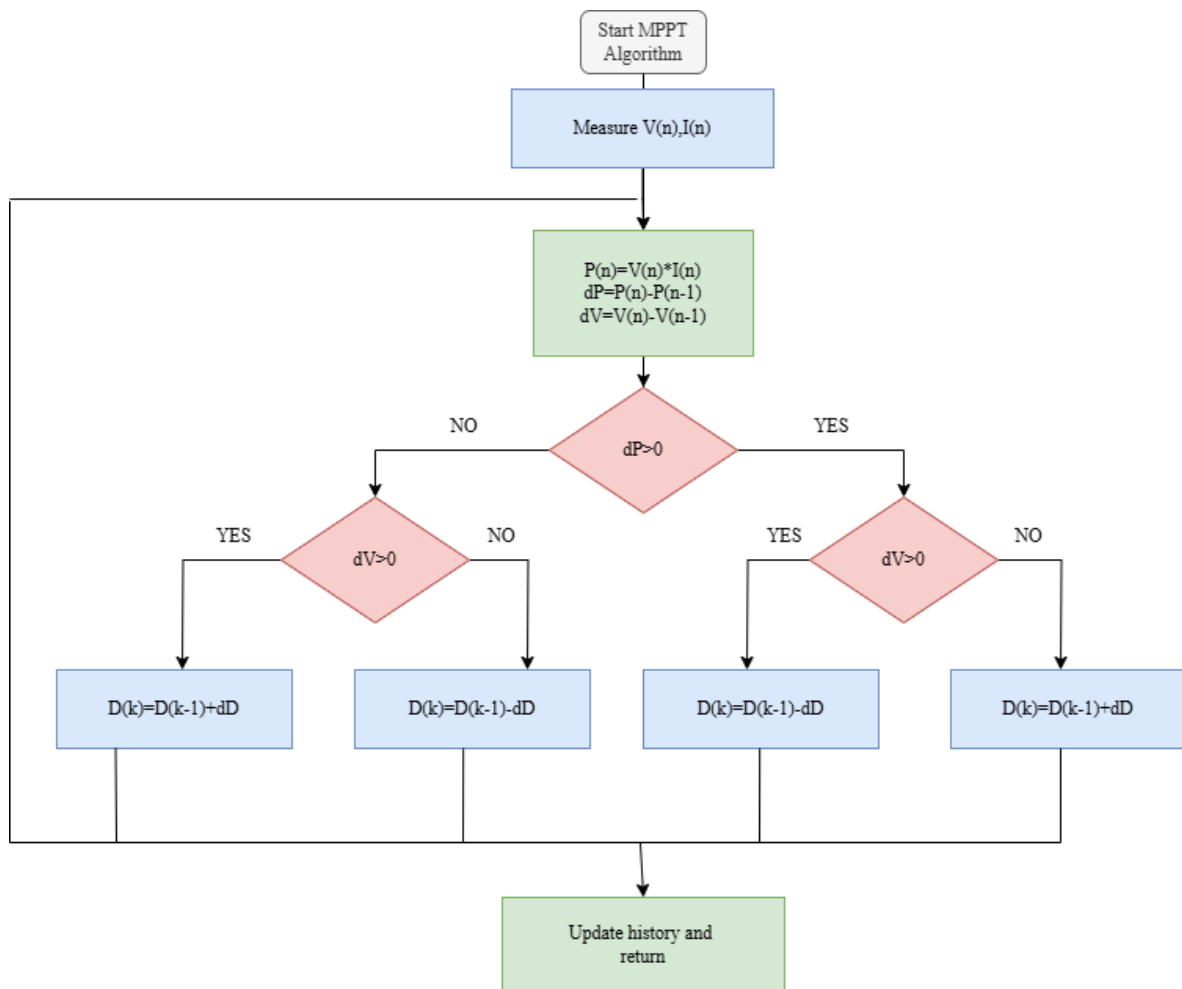


Figure II. 12: The flowchart of the P&O Algorithm.

II.4.3 Perturb & Observe (P&O) Simulation:

We have created the simulation model of the P&O algorithm.

Figure II.13 illustrates SIMULINK's schematic block of the P&O control to track the MPP.

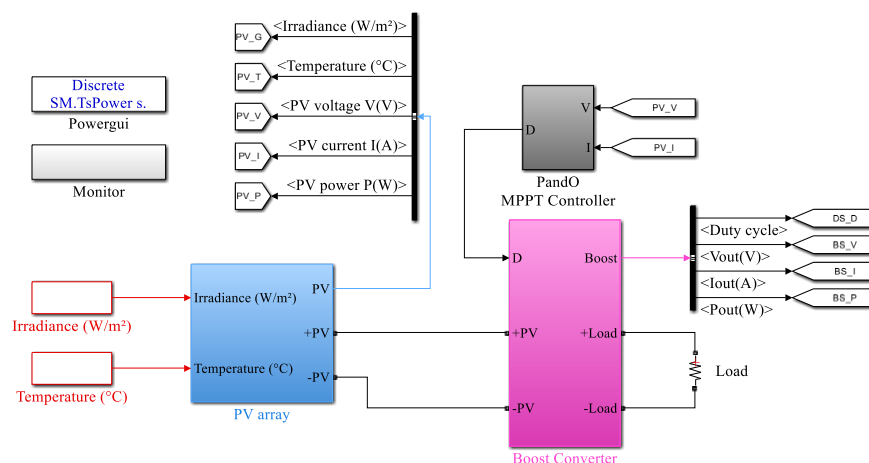


Figure II. 13: Simulation diagram of P&O algorithm.

II.4.4 Simulation results

In this section, we present the simulation for a duration of twenty four seconds. Irradiance and temperature variations are shown in figures II.14 and II.15. The results obtained are represented in figures II.16, II.17, II.18 and II.19, which illustrate the current, voltage, power and duty cycle of the PV system respectively.

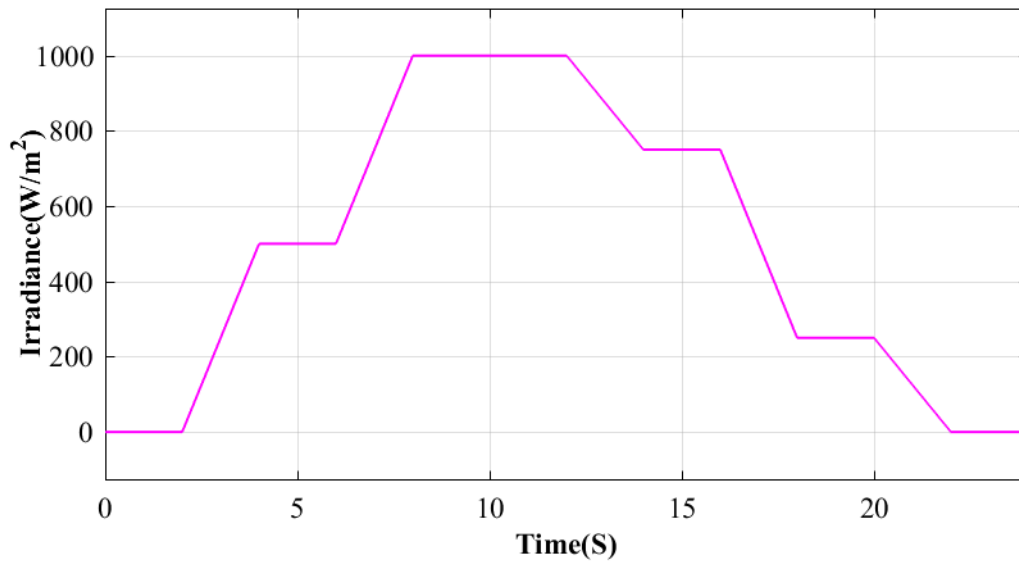


Figure II. 14: Irradiance variations.

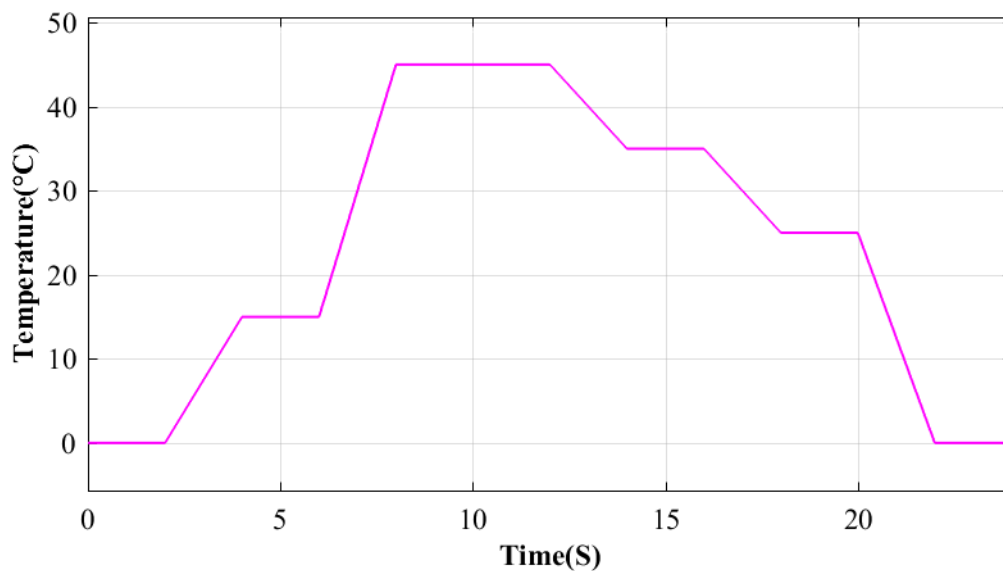


Figure II. 15: Temperature variations.

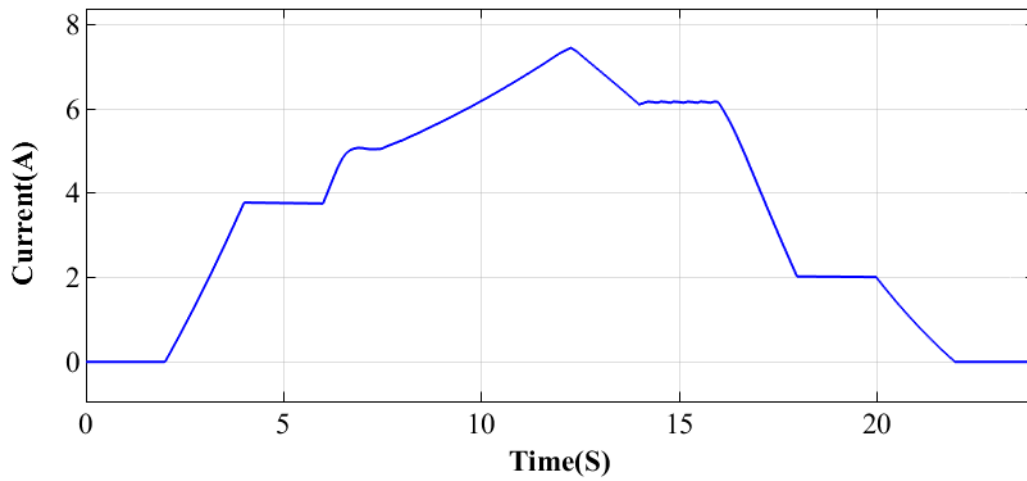


Figure II. 16: Tracking of MPP current by P&O.

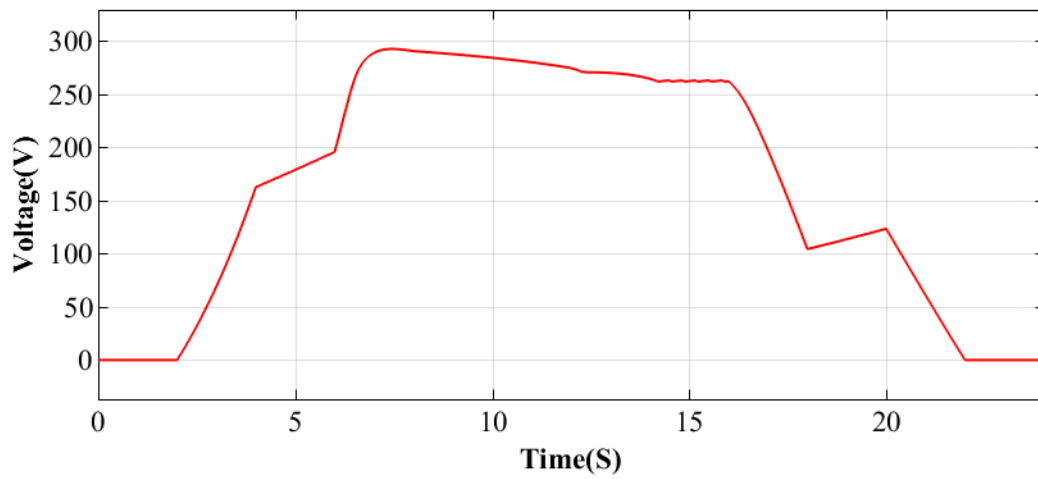


Figure II. 17: Tracking of MPP voltage by P&O.

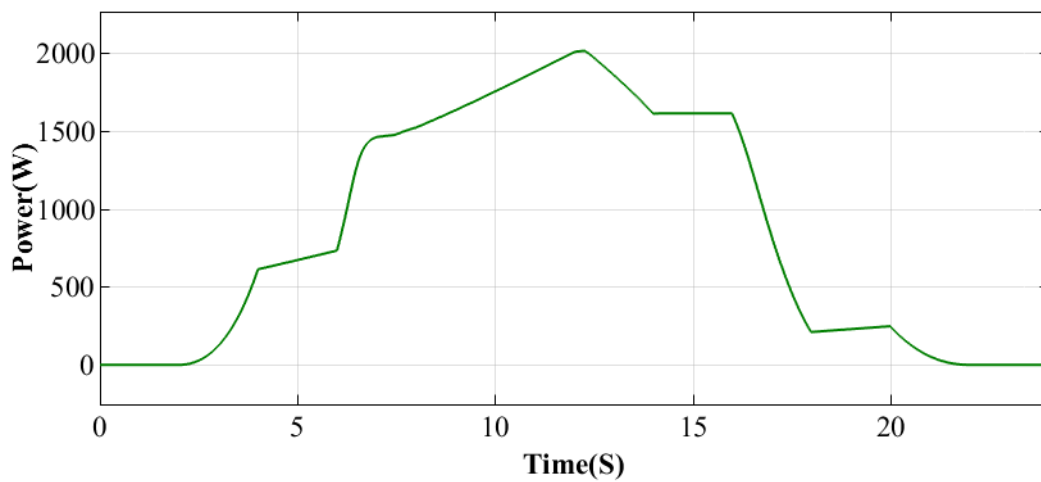


Figure II. 18: Tracking of MPP power by P&O.

Figure II.16: The figure illustrates the PV panel current under the P&O algorithm with varying irradiance and temperature. The PV current from 0 A to the peak of around 7,7 A at $t = 12$ s rises in direct proportion to the rise in irradiance to 1000 W/m^2 . As irradiance drops after $t = 15$ s, current falls progressively back to 0 A. Temperatures as high as 45°C has almost zero direct impact on current, in contrast to voltage. This response shows that the P&O algorithm is successfully using current as a parameter for tracking the MPP.

Figure II.17: The graph shows how the voltage of the photovoltaic panel develops when regulated by the P&O algorithm under varying environmental conditions. PV voltage rises to 290V at about $t = 7$ s, and then kept between 260 V and 280 V as long as irradiance is high ($800\text{--}1000 \text{ W/m}^2$). This is due to the fact that the duty cycle is continuously controlled by the P&O algorithm in order to keep voltage at the MPP. Beyond $t = 15$ s, reduced irradiance and thermal effects result in a sudden drop in voltage to 50V. Temperature, which reaches a high of 45°C , produces a marginal decrease in nominal voltage. With these disturbances not standing still, the system achieves voltage regulation.

Figure II.18: The curve demonstrates that the power accurately follows the variations in irradiance and temperature. It increases with irradiance and reaches a peak around 2010W at $t=12$ s. A noticeable power drop occurs after $t=15$ s, reflecting environmental changes. Additionally, small oscillations appear, which are inherent to the P&O algorithm.

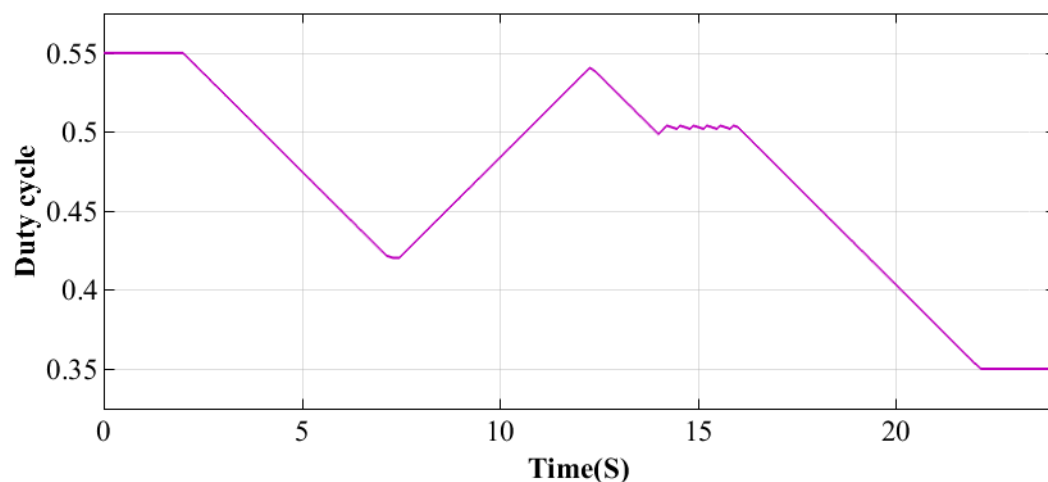


Figure II. 19: Tracking of MPP duty cycle by P&O.

Figure II.19: We set duty cycle in the range 0.35-0.55 to flexibly control the output voltage of boost converter. If irradiance rises up to 1000 W/m^2 at $t = 10$ s the duty cycling self regulates from 0.47 to increase power at maximum point despite the beat due to temperature 45°C . During $t =$

15s, as irradiance is falling down, the duty cycle starts to gradually fall down to 0.35. These variations corroborate the robustness of the P&O algorithm in tracking MPP.

II.5 Conclusion

In this chapter, we have mathematically modeled our solar panel, we have also modeled the analysis of the static DC/DC boost converter. We still need a model that can be used in Simulink. Next, we presented the behavior of our system within the analysis and its performance on the influences of various meteorological parameters, the influence of irradiance and temperature, and visualized the I (V) and P (V) characteristics of the photovoltaic module.

Similarly, MPPT control was demonstrated and these results obtained by the classical P&O method realizing with a PV system. The work was carried out under the Matlab/SimPower environment, and the simulation results proved the effectiveness of this method, but also demonstrated its limitations in terms of rapid convergence and sensitivity to environmental variations. These limitations call for more robust and adaptive approaches, such as artificial intelligence techniques, which will be developed in the next chapter.

Chapter III

ANN and GA-Based MPPT Under Varying and Shaded Conditions

III.1 Introduction

In this chapter, we discuss advanced methods for maximum power point tracking (MPPT) in photovoltaic systems. We begin with the implementation of an artificial neural network (ANN)-based MPPT approach, detailing its key components, system architecture, and simulation results. Thanks to its learning capabilities, the ANN is able to effectively track the MPP even under changing environmental conditions.

Next, we present a genetic algorithm (GA)-based MPPT technique. Its system design, evolutionary optimization process, and simulation outcomes are also described. A performance evaluation is conducted to compare both ANN and GA methods with the conventional Perturb and Observe (P&O) algorithm.

Following an initial comparative study that identified the most effective algorithm for tracking the MPP under varying conditions, a second evaluation was performed under partial shading conditions. In this test, the three algorithms (P&O, ANN, and GA) were assessed and compared to analyze their performance in the presence of multiple maximum power points.

III.2 ANN-based MPPT algorithm

ANN approach is applied on a huge real training dataset to find a PV array's maximum power point [6]. The simulation of the MPPT algorithm based on ANN for a PV system is considered using irradiance and temperature as input and the duty cycle as output.

III.2.1 Principle of training ANN-based MPPT algorithm

As illustrated in the flowchart of figure III.1 .Firstly, we have to run the simulation of the P&O based MPPT algorithm to get the data (input and the target). After that, we start training the ANN. If we reach the required performance, it means the ANN is trained, otherwise, we have to train it again until we get the required performance.

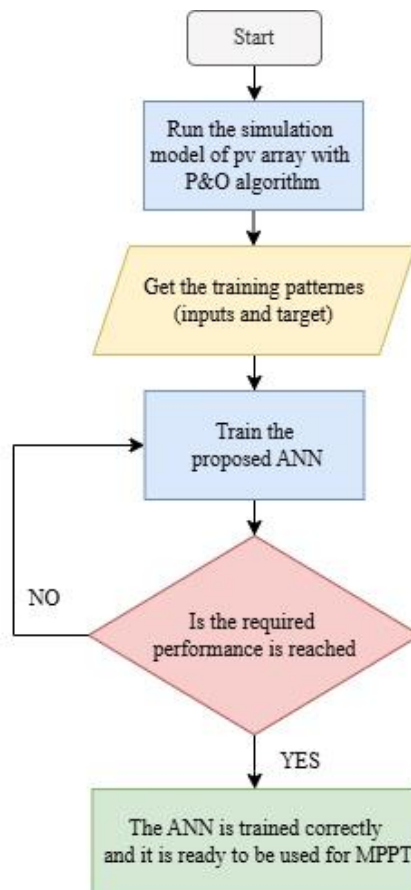


Figure III. 1: Flowchart of the training process of the ANN for MPPT.

III.2.2 Artificial neural network (ANN) simulation

In our work, the MPPT strategy is implemented using an Artificial Neural Network (ANN), where the architecture is illustrated in Figure III.3. This ANN takes as inputs the PV panel voltage and current (2 inputs) and provides as output the duty cycle of the Boost converter. The structure consists of a single hidden layer with 10 neurons, followed by an output layer. The network includes weights (W) and biases (b) in both layers, and is trained to adjust the duty cycle to ensure the panel operates at its Maximum Power Point (MPP).

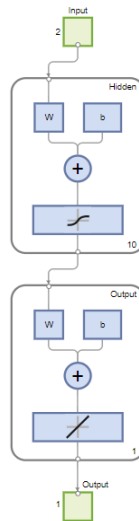


Figure III. 2 : Architecture of the proposed ANN.

We have created the simulation model of the ANN algorithm.

Figure III.2 shows the schematic diagram of the SIMULINK ANN controller for MPP tracking.

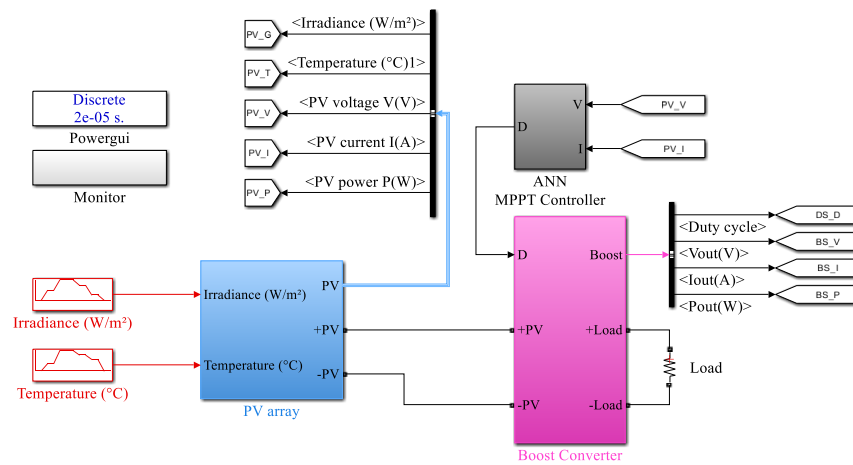


Figure III. 3 : The general diagram of ANN algorithm.

III.2.3 Simulation results

Before presenting the simulation results of our work, we first showed the training results of the ANN algorithm and the resulting block.

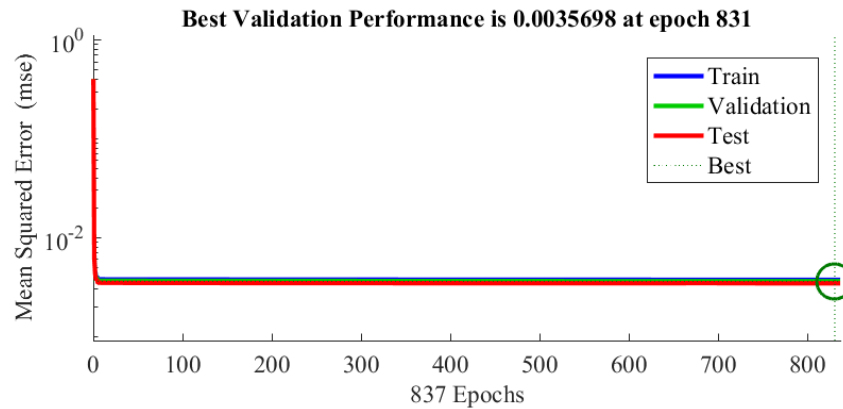


Figure III. 4 :Performance plot of the ANN training.

The performance plot shows the training results of the ANN-based model. As shown in the figure III. 3, MSE converges quickly in the first few iterations and then stabilizes. The minimum error on the validation set is reached at the 831st iteration, with an MSE of 0.0035698. The fact that training, validation, and test curves are in close proximity to each other suggests that the network model is capable of generalizing and does not overfit. The figure III. 5 illustrates how the trained ANN MPPT controller is implemented in Simulink.

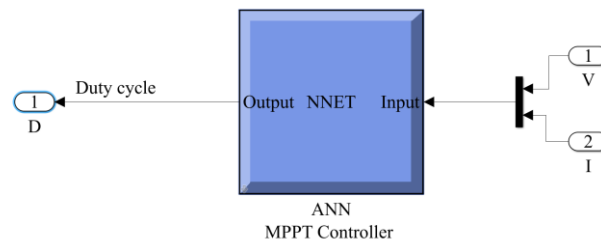


Figure III. 5 : Simulink bloc of the trained ANN MPPT.

We demonstrate the simulation for twenty-four seconds in this part. Temperature and irradiance changes are expressed in figures II.14 and II.15. Figures III.6, III.7, III.8, and III.9, which show the PV system's current, voltage, power, and duty cycle, respectively, illustrate the findings obtained.

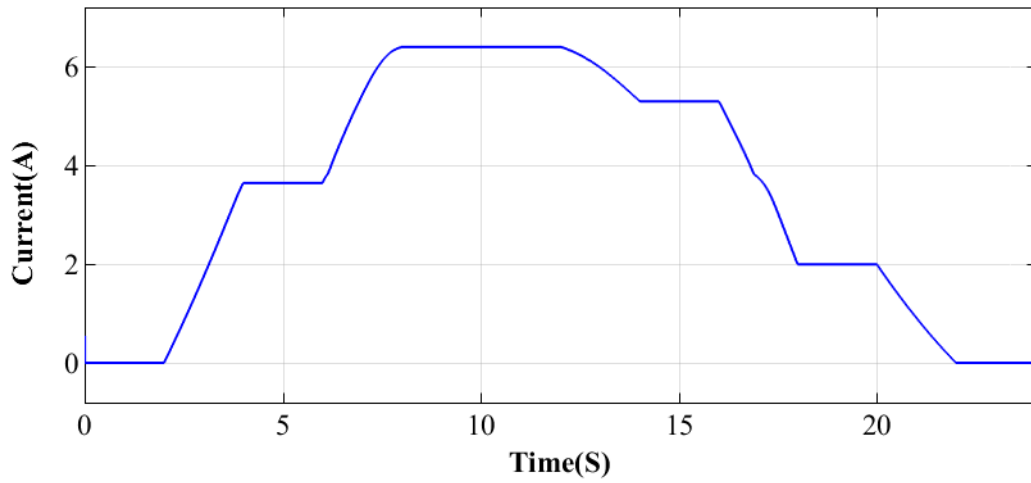


Figure III. 6 : Tracking of MPP current by ANN.

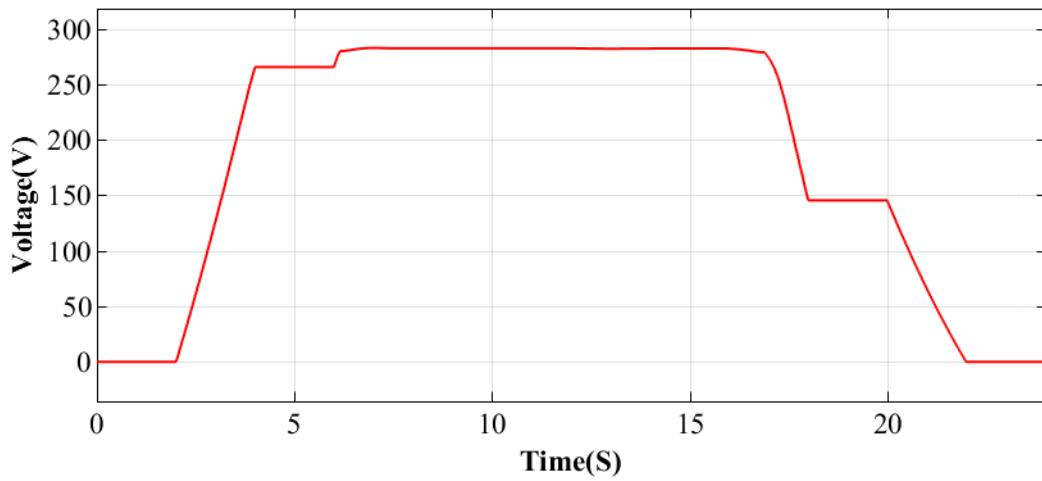


Figure III. 7 : Tracking of MPP voltage by ANN.

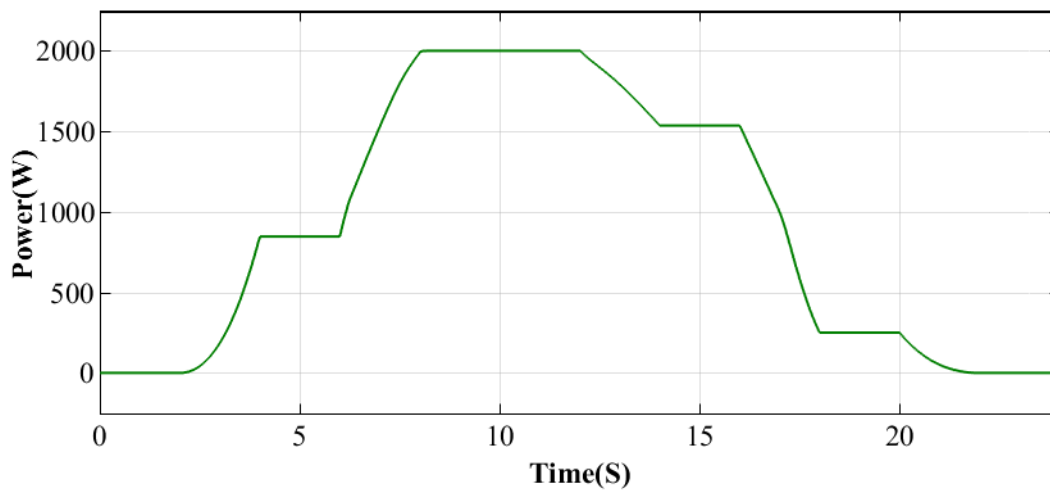


Figure III. 8 : Tracking of MPP power by ANN.

Figure III.6: During the simulation, the output current of the PV module varies between 0 A and 7A. It closely follows the irradiance curve, increasing from 2 A to 7A between $t = 2$ s and $t = 8$ s when the irradiance reaches 1000 W/m^2 . The MPPT algorithm based on ANN is able to quickly search for the optimal point. The effect on the current is minimal when the temperature rises to $45 \text{ }^\circ\text{C}$.

Figure III.7: Under high irradiance, the output voltage reaches a stable level of 270 V between $t = 4$ s and $t = 14$ s. After $t = 15$ s, the output voltage drops to about 80 V as the irradiance decreases. The ANN-based MPPT controller maintains a stable voltage during the optimal operation. High temperatures (above $40 \text{ }^\circ\text{C}$) cause a moderate voltage drop, which is consistent with the expected behavior of PV cells. Overall, the voltage is moderately affected by temperature and is effectively controlled by the ANN controller.

Figure III.8: As the ANN-based MPPT controller rapidly locates and maintains the ideal operating point, the power increases dramatically from $t = 2$ s to $t = 9$ s in which the photovoltaic system reaches its maximum output power of about 1890 W at around $t = 9$ s. The output power rapidly declines as the irradiance reduces after $t = 15$ s, reaching roughly 100 W at $t = 20$ s. Because they lower the voltage, high temperatures result in a minor drop in efficiency.

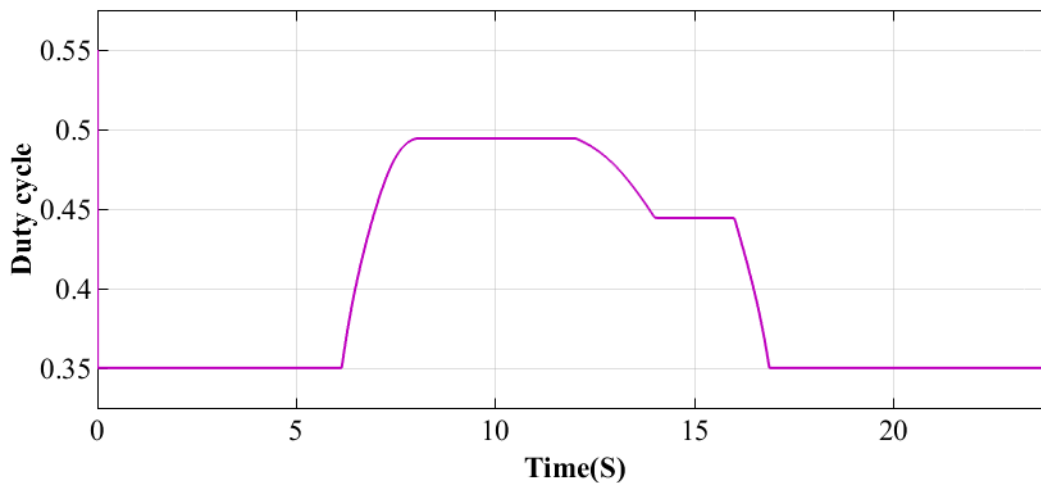


Figure III. 9 : Tracking of MPP duty cycle by ANN.

Figure III.9: The duty cycle fluctuates dynamically between 0.35 and 0.5 during the simulation. To optimize energy transfer, the duty cycle is stabilized to 0.35 when the irradiance is low (around 200 W/m^2). It increases to 0.5 under high irradiance from $t = 6$ s to $t = 14$ s. Even when external conditions vary, the ANN-based MPPT algorithm maintains excellent system efficiency by dynamically adjusting the duty cycle to follow the Maximum Power Point in real time.

III.3 GAs-based MPPT algorithm:

MPPT techniques try to track the optimum point corresponding to the maximum PV power, this point is defined by an optimum current I_{mp} (current at maximum power). By using GAs, one can find this current and keep PV panels working around the maximum power. Figure III.7 depicts the GAs-based MPPT PV system. [5]

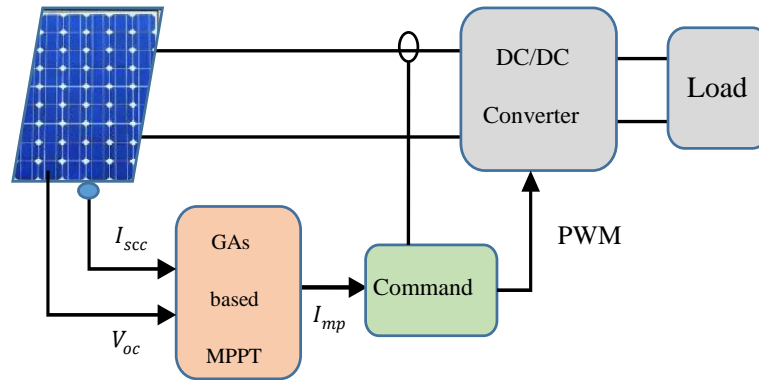


Figure III. 10 : GAs-based MPPT system. [5]

The main idea is to perform genetic transformations (selection, crossover, mutation, and insertion) on a population of individuals in order to finally obtain an optimal individual corresponding to the maximum of a function (fitness function) [5]. The following flow chart (Figure III.8) shows the steps of the algorithm.

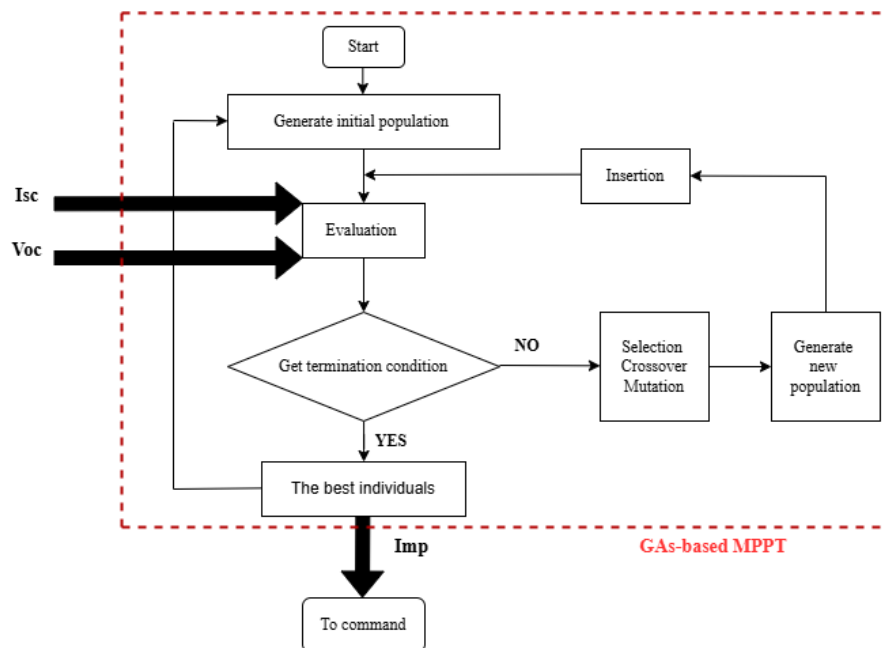


Figure III. 11 : Flow chart of GAs-based MPPT.

A GAs-based MPPT method for PV systems is shown in Figure III.8. It initializes the initial population, evaluates each solution and extract its I_{sc} and V_{oc} , and checks the stopping criterion. If not, the genetic operations (selection, crossover, mutation) generates a new population for re-evaluation. After the optimum solution is determined, this solution is applied and sent to the system controller in order to work at the MPP.

III.3.1 Genetic algorithms (GA) simulation

We have created the simulation model of the P&O algorithm.

Figure II.9 illustrates SIMULINK's schematic block of the P&O control to track the MPP.

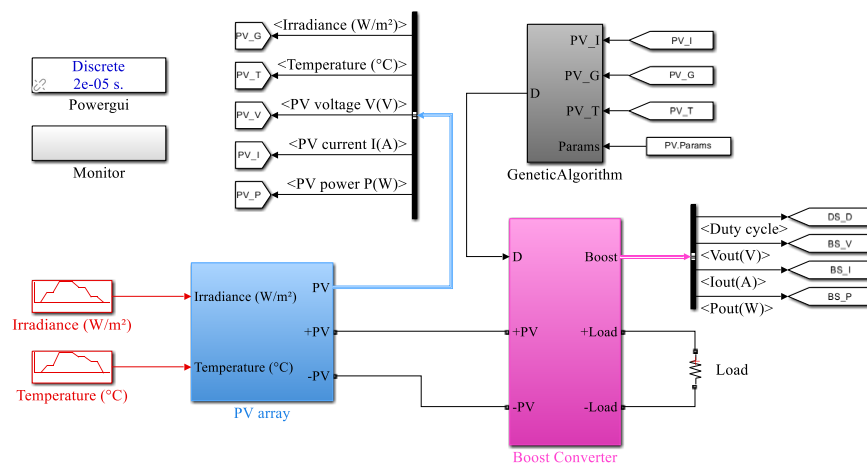


Figure III. 12 : The general diagram of GAs algorithm.

III.3.2 Simulation results

In this section, we present the simulation results over a period of twenty-four seconds. The variations in temperature and irradiance are shown in Figures II.14 and II.15. The results obtained are illustrated in Figures III.13 to III.16, which display the PV system's current, voltage, power, and duty cycle, respectively.

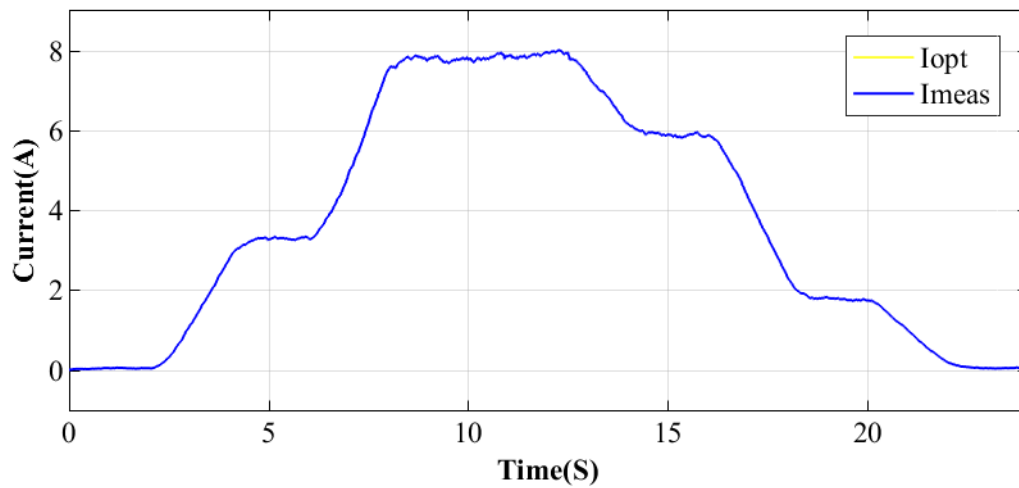


Figure III. 13 : Tracking of MPP current by GA.

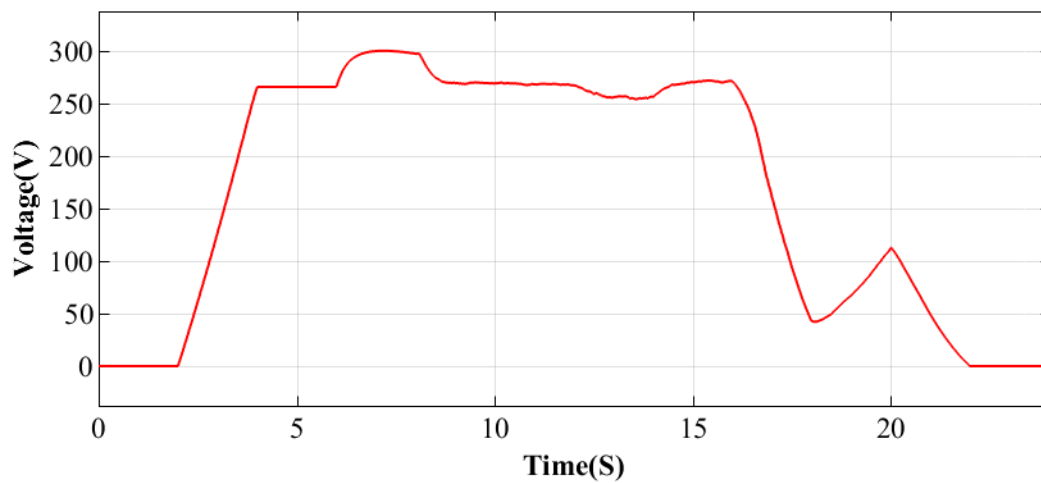


Figure III. 14 : Tracking of MPP voltage by GA.

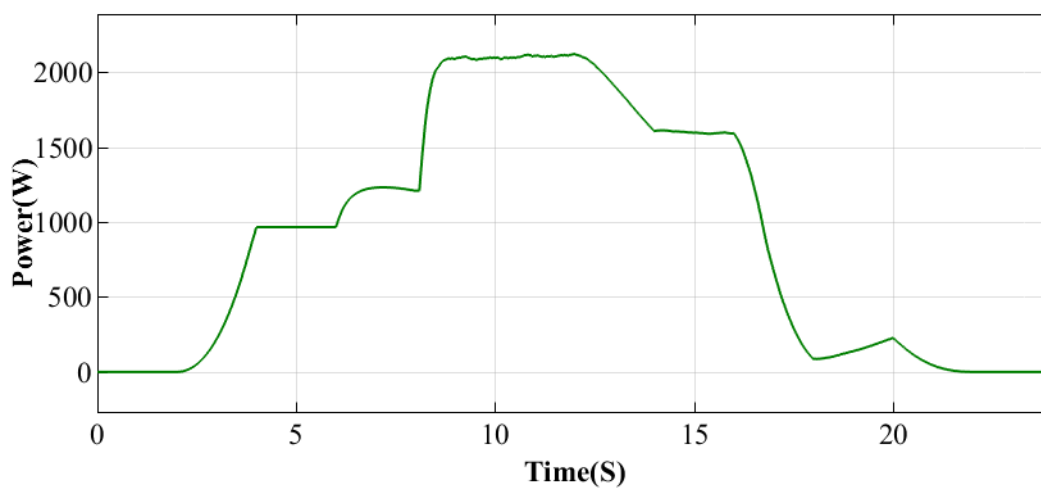


Figure III. 15 : Tracking of MPP power by GA.

Figure III.13: The genetic algorithm shows excellent performance in tracking the maximum power point. It manages to find the optimal current values that match the changing sunlight conditions — reaching about 8 A around 10 seconds when irradiance is high, and gradually decreasing to 0 A by 22 seconds as sunlight drops. The fact that the optimized current (I_{opt}) perfectly follows the actual measured current (I_{meas}) means the algorithm works efficiently and accurately. This confirms the GA's strong ability to provide reliable and adaptive control for maximizing energy extraction in real time.

Figure III.14: In the first several seconds, PV voltage rapidly climbs to 270 V, peaking at nearly 300 V at about 7 s, and slightly decreases to approximately 260 V even under the constant irradiance with the temperature increased to 45°C. Irradiances decrease causing a sharp decline to 50 V after 15 s. Voltage is strongly temperature-dependent, and the GA dynamically controls the duty cycle to compensate.

Figure III.15: PV power is maximum of approximately 2100 W between 7s and 12s at an irradiance of 1000 W/m² and approximately 35–40°C. Power decreases to approximately 1200 W when irradiance is dropped to 600 W/m², and it goes down to 0 W towards the termination. Elevated temperature (~45°C) causes minimal loss of power due to voltage drop. The genetic algorithm successfully maximizes the extracted power by real-time adaptation of converter parameters.

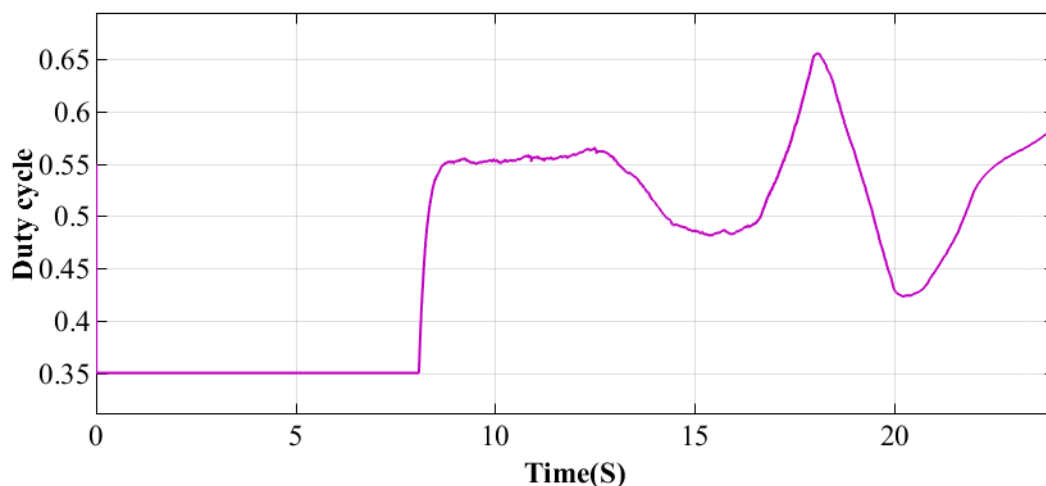


Figure III. 16 : Tracking of MPP duty cycle by GA.

Figure III.16: The duty cycle lies between 0.35 and 0.65 depending on temperature and irradiance. The duty cycle rises in a gradual manner up to a level of approximately 0.55 with higher

irradiance for efficient energy transfer. After 15s, there is a high slope up to 0.65 to maintain voltage in low irradiance. This control shows the effectiveness of GA for MPPT.

III.4 Partial shading based MPPT algorithms

In this work, we focus on the challenge of MPPT under partial shading conditions. By applying different algorithms — such as P&O, ANN, and GA — we aim to evaluate which one performs best in optimizing energy extraction from the PV system when shading occurs.

III.4.1 Testing partial shading model

A simulation model was developed to analyze the behavior of a PV system exposed to varying irradiance levels: 1000, 600, and 300 W/m² at 25°C. The three PV arrays are connected in series, allowing us to replicate realistic partial shading conditions. Figure III.17 expressed the phenomenon.

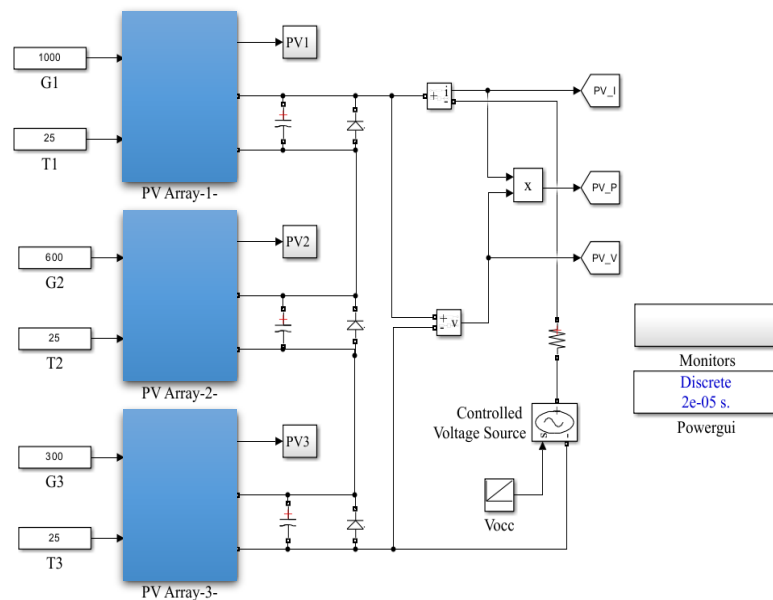


Figure III. 17 : Partial shading test setup.

The I-V curve show in Figure III.18 illustrates a noticeable steps caused by the activation of bypass diodes, which occur when some solar cells receive less sunlight than others. These steps reflect sudden drops in current at specific voltage levels. While Figure III.19 represents the corresponding P-V curve which displays multiple peaks, making it more difficult to locate the true Maximum Power Point (MPP). In this case, the MPP is found at 189.27 V and 4.48 A, giving a maximum power output of 847.32 W.

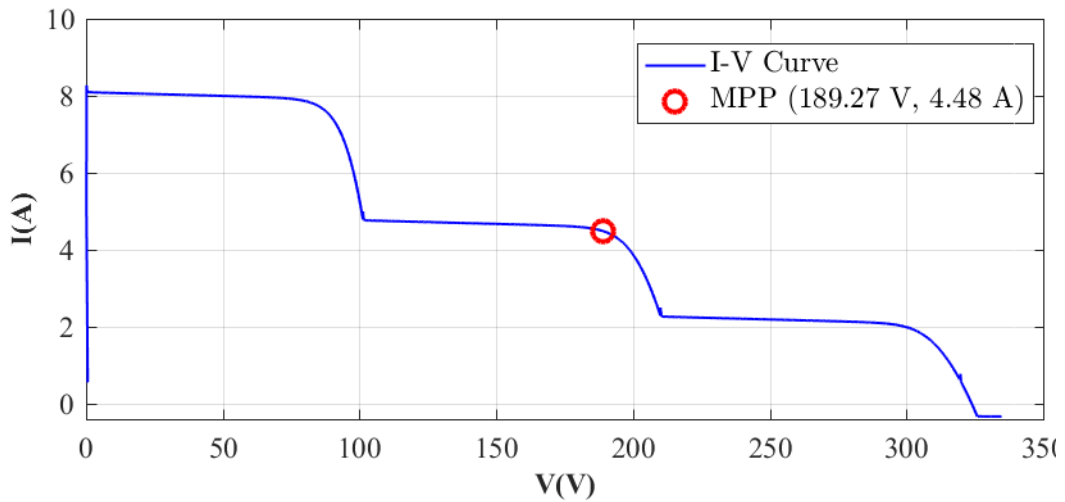


Figure III. 18: I-V characteristics of PV under partial shading .

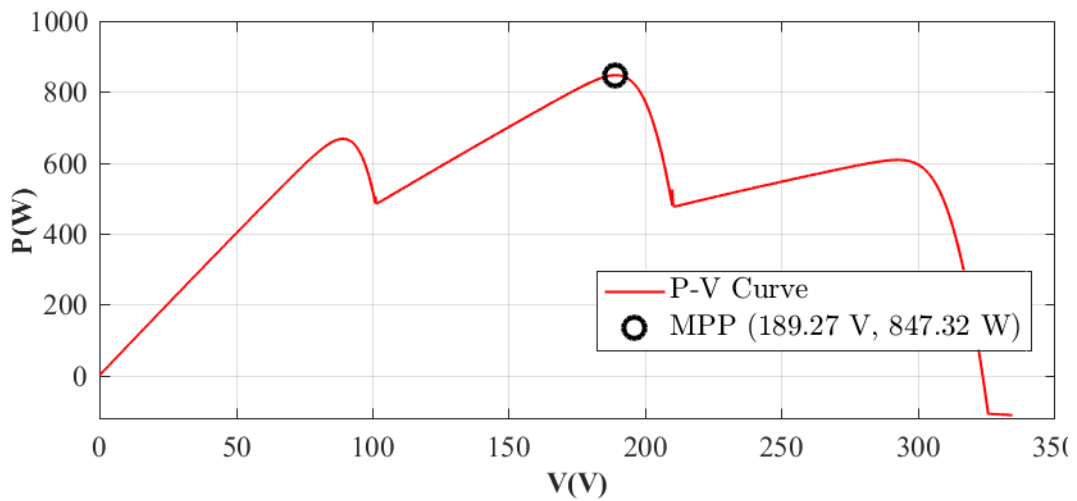


Figure III. 19: P-V characteristics of PV under partial shading .

To enhance energy extraction, several MPPT algorithms, including GA, ANN, and P&O, were implemented. The resulting performance in terms of current, voltage, and power under partial shading will be presented in the comparative study.

III.5 Comparative performance study

To better understand the performance of the three MPPT algorithms, we divided our comparison into two key parts. First, we compare their behavior under normal conditions, then under partial shading. This approach gives a complete and realistic view of their efficiency and reliability.

III.5.1 Under normal conditions

We evaluate the performance of MPPT algorithms — P&O, ANN, and GA — applied to a PV system under varying irradiance and temperature conditions by analyzing voltage (figureIII.20), current (figureIII.21), power (figureIII.22), and the instantaneous power error (figureIII.23). This allows for a clear assessment of each algorithm's accuracy and robustness.

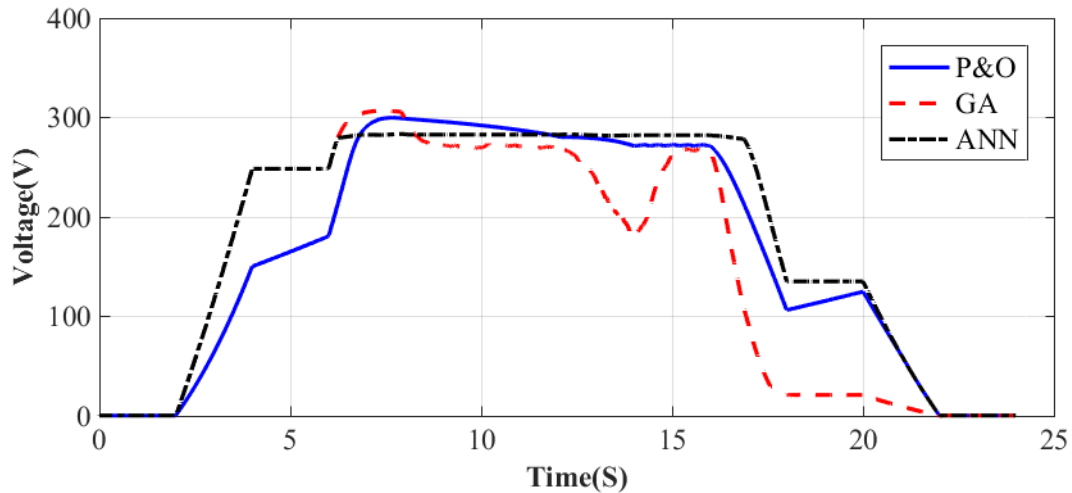


Figure III. 20 : PV voltage comparison under normal conditions.

The GA algorithm achieves the most accurate and stable voltage output, reaching 273 V, which closely matches the nominal value of 272.9 V, without significant oscillations. The ANN also performs well, with a similar peak but minor fluctuations between 12 and 15 seconds. In contrast, the P&O algorithm peaks at a lower 270 V and shows more oscillations and slower response. Thus, GA is the most effective, followed by ANN, while P&O is the least accurate and stable.

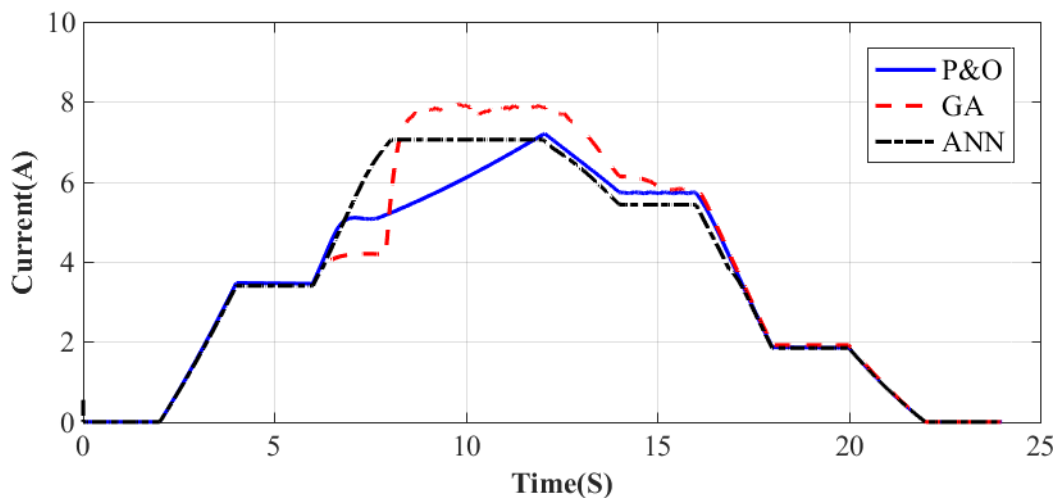


Figure III. 21 : PV current comparison under normal conditions.

The current output also confirms the superiority of the GA algorithm. It reaches a peak of 7.7 A at $t=9s$, which is nearly equal to the nominal value of 7.71 A. The ANN follows with about 7.5 A and shows good stability. In contrast, P&O peaks at only 7.4 A, with more fluctuations and slower response. Overall, GA performs best, followed by ANN, while P&O is the least effective.

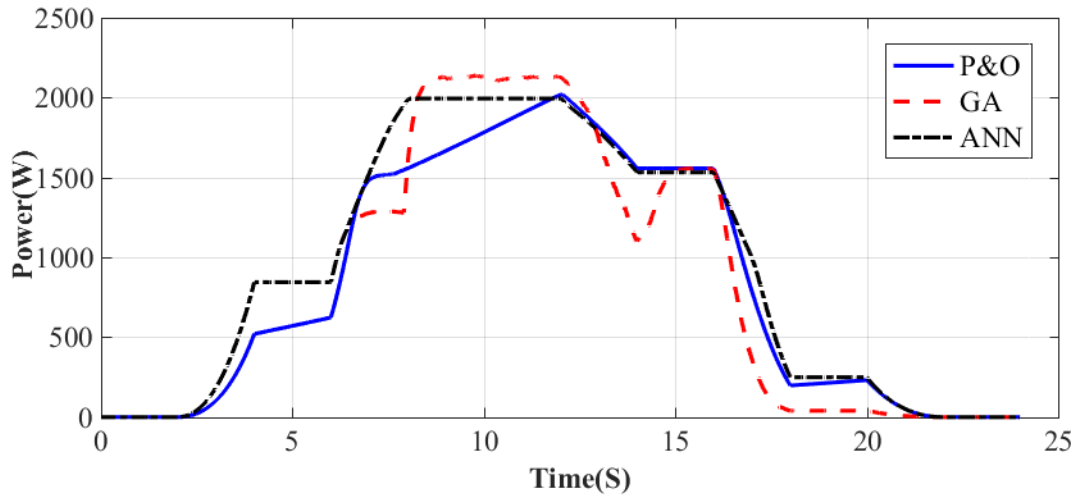


Figure III. 22 : PV power comparison under normal conditions.

The GA algorithm delivers the best performance, reaching 2123 W, which exceeds the nominal power of 2105.36 W, and maintains excellent stability even under varying irradiance levels. It responds quickly to changes in sunlight without significant power loss. The ANN reaches 1980 W with decent performance, but slight oscillations appear during irradiance transitions. In contrast, P&O peaks at only 1900 W and struggles to maintain stable output during fluctuations in irradiance. Overall, GA proves to be the most efficient and robust under dynamic environmental conditions.

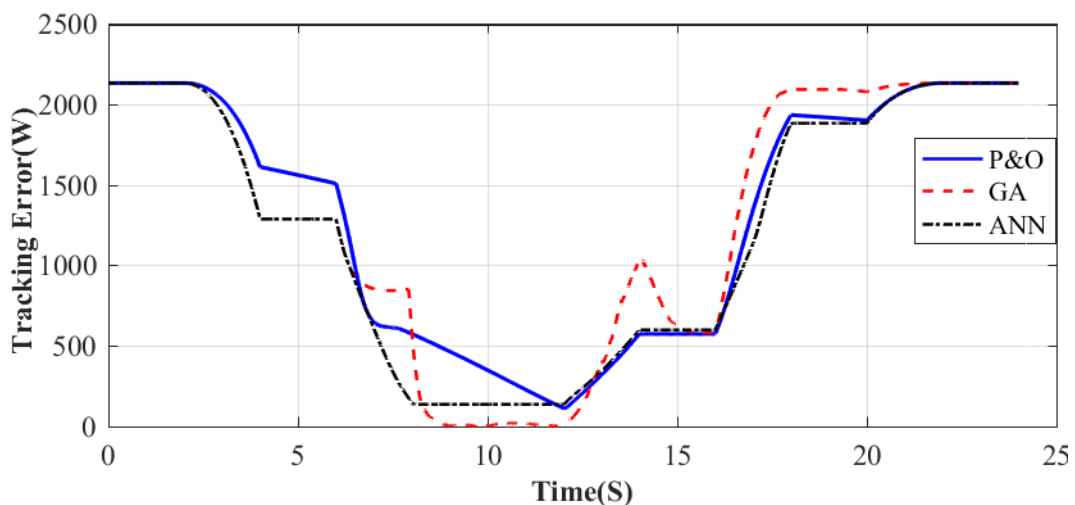


Figure III. 23 : Instantaneous MPPT tracking error under normal conditions.

This figure clearly compares how the three algorithms respond to changing irradiance and temperature. The GA algorithm shows the most accurate and robust performance, keeping the error near zero between 8 and 13 seconds. It has a small peak around 14 seconds (~900 W), which is likely due to a sudden change in environmental conditions that temporarily disturbs the tracking. GA quickly re-adapts, thanks to its fast convergence. The ANN is more stable than P&O, maintaining a consistent error of 300–500 W, but it remains less precise than GA. The P&O method is the least effective, showing a slow response, especially between 0–5 s and 17–20 s. Overall, GA stands out for its speed, accuracy, and adaptability, making it the most reliable algorithm in dynamic conditions.

III.5.2 Under partial shading

To examine the impact of partial shading on MPPT performance, the P&O, ANN, and GA algorithms were individually implemented on a PV system. Their behavior was analyzed through voltage, current, power output, and instantaneous power error, as illustrated in Figures III.24 to III.27. This comparison highlights how each method performs in terms of precision and reliability in maximum power point tracking.

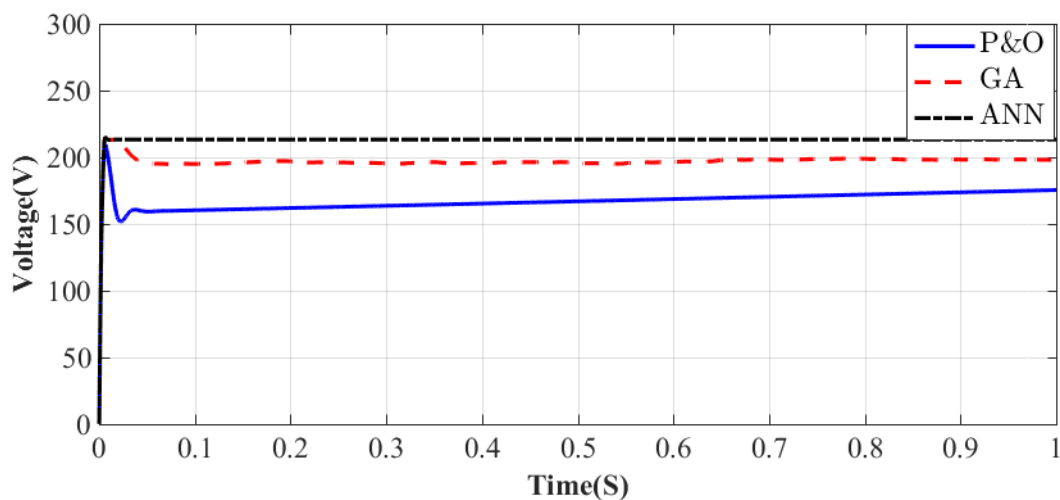


Figure III. 24 : PV voltage comparison under partial shading conditions.

In the critical interval [0.2 s – 0.4 s], the GA algorithm reaches a voltage of 195 V, very close to the nominal value of 189 V, with good stability. The ANN overshoots significantly, reaching 213 V, indicating poor MPP tracking. P&O falls short with 165 V, far below the expected level. GA proves to be the most accurate and stable, followed by P&O, while ANN performs poorly in terms of voltage accuracy.

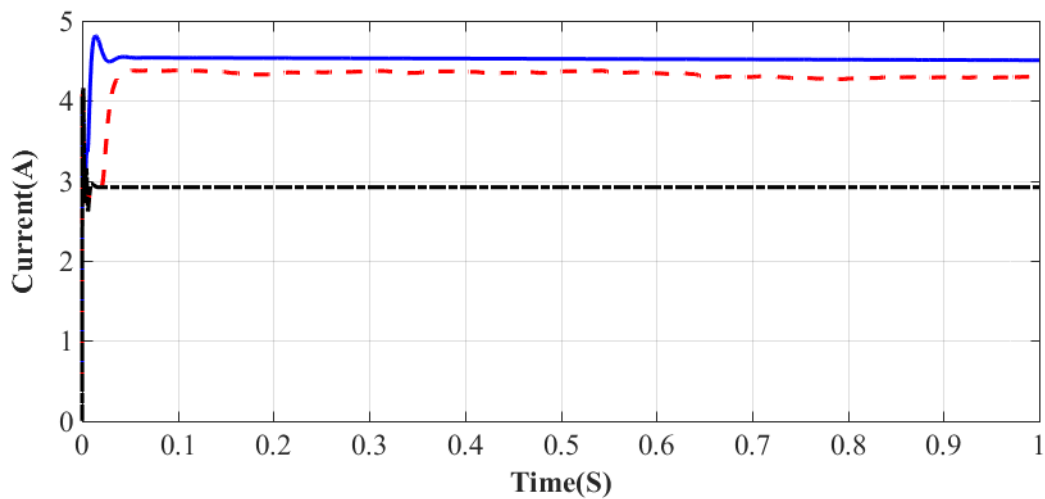


Figure III. 25 : PV current comparison under partial shading conditions.

Within the same 0.2 s to 0.4 s window, P&O produces the highest current (4.52 A), but when combined with low voltage, it doesn't yield optimal power. The GA reaches 4.36 A, showing a well-balanced voltage-current output, resulting in efficient performance. ANN falls behind with only 2.92 A, indicating poor adaptation to the optimal operating point. GA again shows the best balance and tracking performance, followed by P&O, with ANN being the least effective.

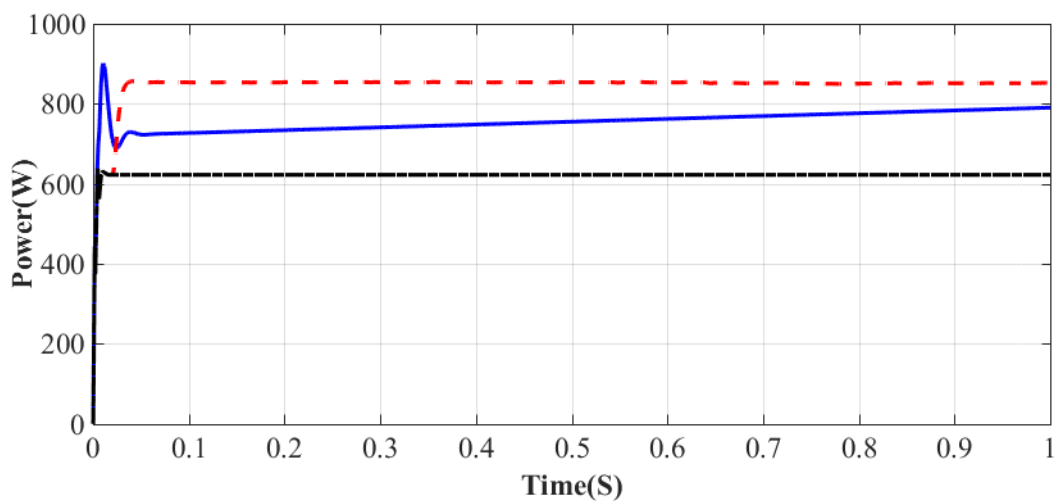


Figure III. 26 : PV power comparison under partial shading conditions.

During this interval, the GA delivers 853 W, exceeding the nominal power of 847.32 W, with excellent stability under partial shading. P&O achieves 748 W (~88%), which is acceptable but not optimal. ANN outputs only 622 W (~73.4%), which is significantly lower, showing ineffective power tracking. GA clearly stands out as the most efficient and robust algorithm.

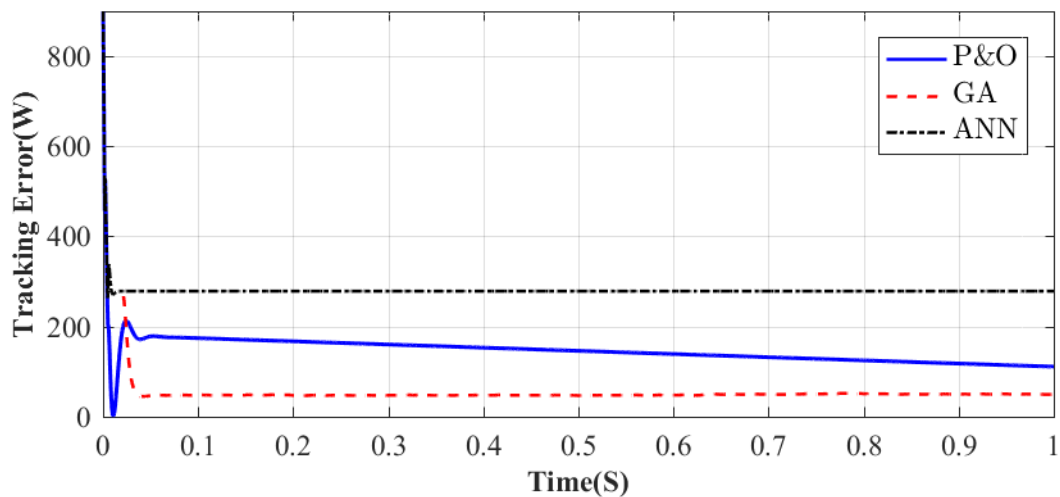


Figure III. 27 : Instantaneous MPPT tracking error under partial shading.

The instantaneous power error under partial shading clearly shows that the GA algorithm performs best, maintaining an error that is very low and nearly flat, especially between 0.2 s and 0.4 s. This confirms its speed, precision, and strong robustness, consistent with its high power output of 853 W. The P&O algorithm shows a moderate error of about 190 W, which indicates a slower response but still acceptable tracking. In contrast, the ANN algorithm reaches the highest error, around 300 W, showing that it has trouble keeping up with the MPP under shading. These results clearly validate that GA is the most efficient and reliable method in challenging conditions.

Table III.1 showing the performance of the three MPPT algorithms (GA, ANN, and P&O) under both normal conditions and partial shading, based on three key criteria: rapidity, effectiveness, and robustness.

Table III. 1: Comparative performance study of MPPT techniques.

Algorithms	Test conditions	Rapidity	Effectiveness	Robustness
GA	Normal	Very fast	Very high	Excellent
	Partial shading	Fast	High	Very good
ANN	Normal	Medium	Medium	Medium
	Partial shading	Slow	Low	Low
P&O	Normal	Slow	Low	Medium
	Partial shading	Very slow	Medium	Low

III.5 Conclusion

This work has explored various methodologies MPPT for photovoltaic systems. The ANN-based and GA-based MPPT methods were executed and assessed through simulation first. According to the comparison outcomes, GA algorithm outperformed other algorithms in terms of tracking precision, convergence time, and overall system stability. In addition, the robustness of the GA-based MPPT under partial shading was remarkable, avoiding local peak traps and ensuring maximal power extraction. These simulation results confirm the importance of smart optimization strategies in improving the performance of PV systems.

These strategic goals will be pursued in the following chapter, which will concentrate on the real-time application and testing of the proposed MPPT control methods, especially the P&O method as a starting point.

Chapter IV

***Experimental Validation of MPPT Control for PV
Systems Using dSPACE***

IV.1 Introduction

This final chapter focuses on the implementation of a photovoltaic system and the real-time evaluation of the performance of the Perturb and Observe (P&O) algorithm using the dSPACE 1104 card.

dSPACE boards are used for real-time control based on models developed in MATLAB/Simulink. They allow graphical problem-solving through the “ControlDesk” operating software, which significantly reduces development and prototyping time for control systems [38].

IV. 2 Presentation of DSPACE 1104

The DS1104 is a powerful control board for rapid prototyping controllers. Its computing power and inputs/outputs are essential for applications involving numerous actuators and sensors. It can be programmed using the Matlab Simulink environment. A DSPACE product, it consists of two parts: [38]

- An interface card equipped with a DSP processor linking the control panel to the computer. It enables data to be acquired and processed on the computer.
- A control panel with BNC sockets for converting analog data to digital and other sockets delivering analog and digital signals from the card. There are also PWM connections, a digital input/output connection, two RS232 and RS422 serial connections, and two other connections for an encoder.



Figure IV. 1 : Connection panel for DSPACE 1104.

IV.2.1 dSPACE 1104 Inputs/Outputs

The interface of the dSPACE 1104 card comprises several input/output modules, as shown in the figure below: [39]

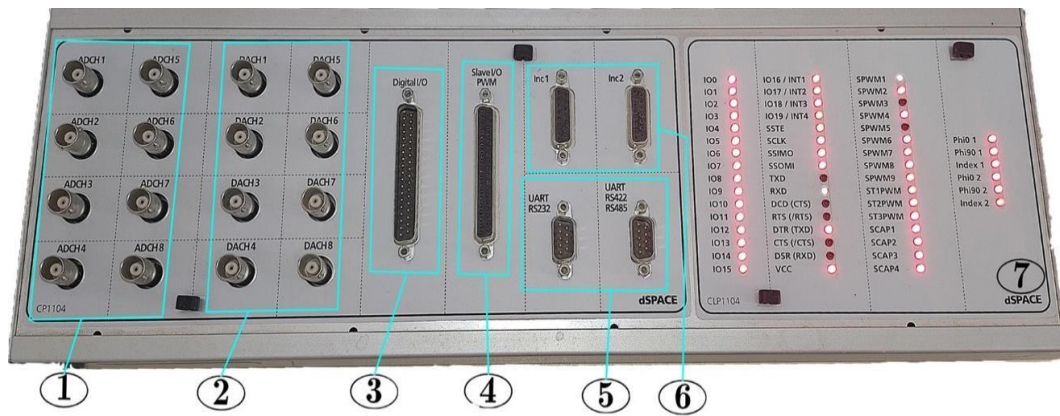


Figure IV. 2 : Construction of the dSPACE 1104 serial interface .

- (1) eight analog-to-digital converters (ADCs), 1, 2, 3, 4 in 12 bits and 5, 6, 7, 8 in 16 bits.: used to retrieve analog data from a system, then convert it to digital and display it on a PC.
- (2) eight 16-bit digital-to-analog converters (DACs) capable of delivering a voltage of ± 10 V, used to convert digital data input from the PC into analog data, and then feed it into an external system.
- (3) Digital input/output is used when dealing with a programming language.
- (4) Input/output of the slave DSP responsible for generating PWM signals for inverter control.
- (5) Serial ports (RS 232, RS 422, and RS 485): used for serial communication between the dSPACE 1104 and various electronic devices (automat, measuring device, etc.). They also ensure communication between two dSPACE cards.
- (6) two incremental encoders for retrieving data from sensors (position sensors).
- (7) Equally adorned are some forty LED lights indicating which doors are active on the

Panel .[38]

IV.2.2 Control Desk

It's an interface that lets you visualize in real time the different variables in the file developed in Simulink.[39]

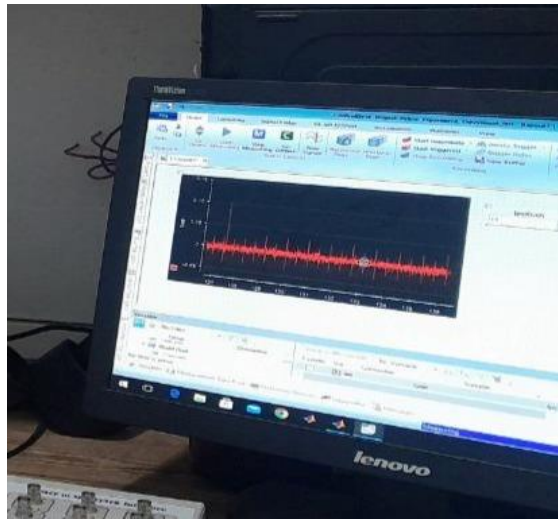


Figure IV. 3 : Control Desk interface.

IV.3 realization of the electronic circuit

The experimental work was carried out in the L2GEGI laboratory (Laboratoire de Génie Énergétique et Génie Informatique) at Ibn Khaldoun University, Tiaret.

Figure IV.4 illustrates the panel used in our project, while Figure IV.5 presents the final implementation with all components clearly numbered.



Figure IV. 4 : DIMEL SOLAR Panel.

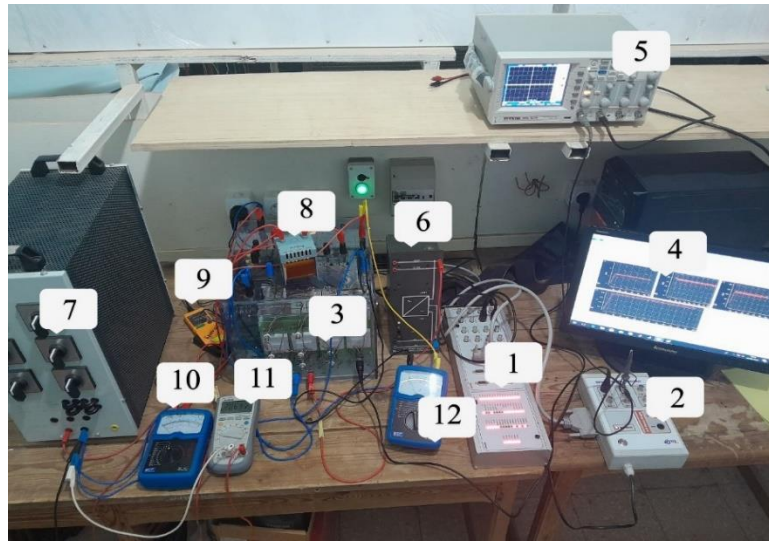


Figure IV. 5 : The experimental PV system .

The numbers corresponding to the components of figure IV.5 are listed in Table IV.1.

Table IV. 1 : Components of realization .

Numbers	Components
1	DSPACE 1104
2	insulation card
3	Boost converter
4	Control Desk
5	Oscilloscope
6	continuous supply
7	Load
8	Coil
9	current sensor
10	ampere meter
11	multimeter
12	voltmeter

IV.4 Realization results

Our experimental work was carried out in two stages: an initial test to verify the operation of the boost converter, followed by a second test focusing on the implementation of the P&O algorithm for Maximum Power Point Tracking (MPPT).

IV.4.1 Test of Boost converter

Before connecting the photovoltaic panel, we tested the boost converter using a 15 V DC power supply to verify its performance. Figure IV.6 presents the finding results.

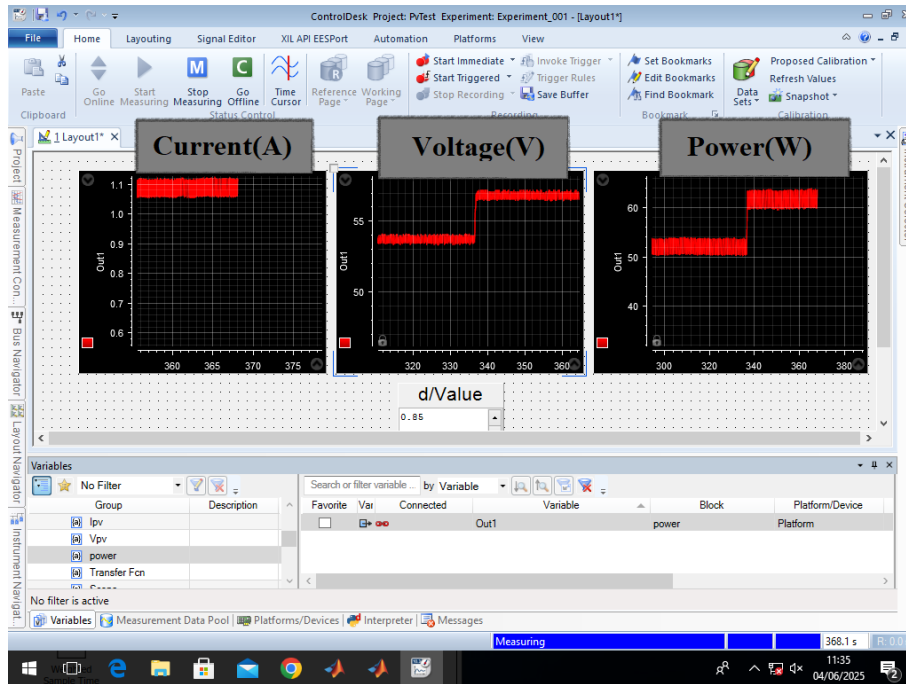


Figure IV. 6 : Electrical Response of the Converter During Testing.

The results showed that the current quickly stabilized around 1.1 A, while the voltage increased gradually to reach about 60 V. As a result, the output power rose to nearly 65 W. This behavior confirms that the converter operates correctly in boost mode, with good efficiency. The test also demonstrated the system's ability to respond dynamically, proving it is ready for the next phase with the solar panel.

IV.4.2 Implementation of the P&O algorithm

After validating the operation of the converter, we powered the system using an 80 W photovoltaic panel and applied the P&O algorithm for Maximum Power Point Tracking (MPPT). The tests were conducted on June 4, 2025, at 12:30 p.m., under very low irradiance and temperature, below standard operating conditions.

The figure IV.7 presents the experimental curves of the current, voltage, power, and duty cycle of the boost converter.

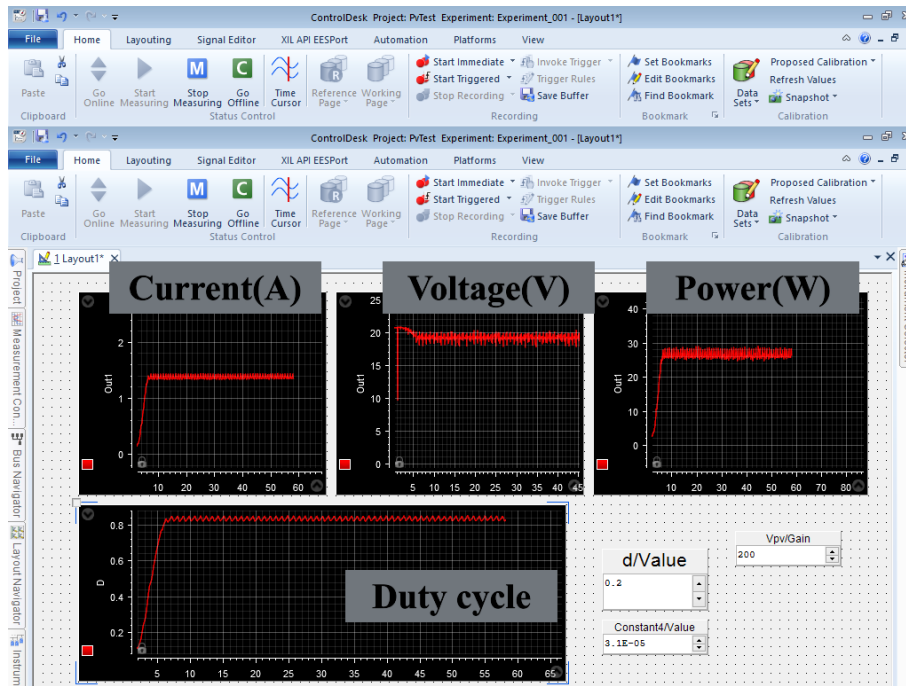


Figure IV. 7 : Experimental Results of P&O Algorithm Implementation .

- The output current quickly stabilizes at around 1.4 A. This fast transient response indicates the effectiveness of the P&O algorithm in adjusting the converter's operating point, even under low irradiance conditions. The absence of significant oscillations confirms the system's stability and reliability.
- The output voltage stabilizes at approximately 19 V after a brief transient phase. This value is consistent with the panel's behavior under reduced irradiance, demonstrating that the converter successfully regulates the voltage to maintain operation near the MPP.
- The system's extracted power reaches about 29 W, which is reasonable given the actual test conditions (irradiance $< 1000 \text{ W/m}^2$). This trend confirms effective MPP tracking, with good stability and minimal oscillations around the optimum point.
- The duty cycle quickly converges to a stable value of approximately 0.82, meaning the converter operates at 82% of its switching period to optimize power extraction. This effective duty cycle regulation reflects a robust control behavior ensured by the P&O algorithm.

IV.5 Conclusion

This chapter was devoted to the practical implementation of our project, starting with the presentation of the DSPACE card, a powerful tool for real-time control applications. Then we described the Control Desk software, which provides a user-friendly interface for monitoring, controlling, and analyzing the system performance. In the implementation phase, we used the P&O

(Perturb and Observe) algorithm to track the maximum power point. Although this algorithm is efficient and easy to implement, it is sensitive to rapid changes in climatic conditions, which limits its robustness. However, the experimental results confirmed the correct function of the system. We successfully completed all stages of our work with due diligence. This project provides a solid foundation that, inshallah, can be further developed and improved in the near future.

General conclusion

This thesis is set in the renewable energy production sector, specifically the improvement of photovoltaic systems through maximum power point tracking (MPPT). The crucial objective was to evaluate the performance of the Genetic Algorithm (GA) in the context of MPPT, comparing it in parallel with other conventional and intelligent methods.

In the first chapter, we introduced photovoltaic systems, covering the basics of solar energy, the operation of the PV cell, and the advantages and disadvantages of PV systems. We also introduced DC-DC converters and MPPT control, as well as the main techniques: P&O, ANN, and GA. In addition, we introduced the phenomenon of partial shading.

Chapter Two was devoted to the modeling and simulation of a photovoltaic system using Matlab/Simulink. We applied the conventional P&O algorithm, analyzed its operating principle and interpreted the results to assess its performance.

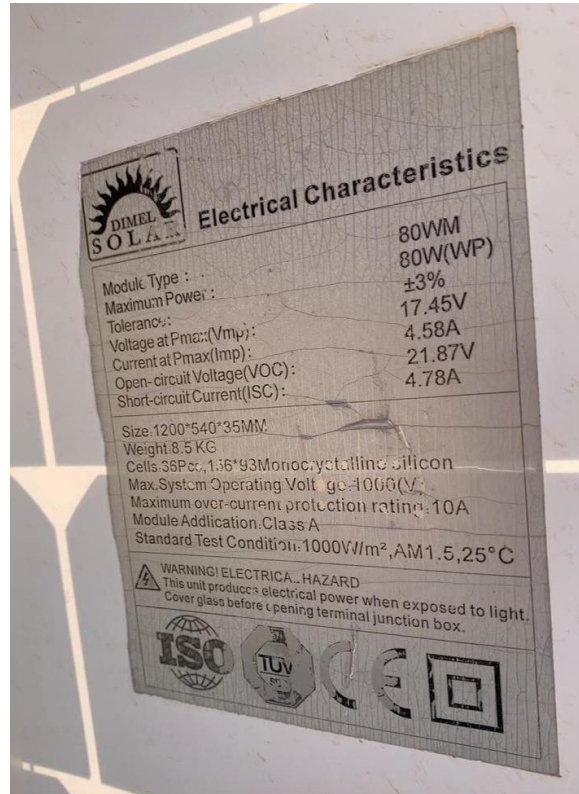
In chapter three, we developed two intelligent MPPT techniques: neural networks (ANN) and the genetic algorithm (GA). then simulated in various scenarios, including partial shade. A comparative analysis of the P&O, ANN and GA methods is followed by a detailed discussion of the results.

Finally, the fourth chapter was devoted to the experimental realization of a photovoltaic system using the DSPACE 1104 card. After an introduction to the board and its development environment (Control Desk), tests were carried out on the boost converter. The platform integrated the P&O method, and the experimental results were analyzed to confirm that the system was in good working order.

In conclusion, the genetic algorithm (GA) stood out as the most effective method for monitoring MPP, particularly in the case of partial shading, thanks to its robustness and adaptability. Despite this, its complexity and high computation time limit its use in real time. This work confirms the potential of intelligent algorithms and paves the way for future research to facilitate their integration into grid-connected PV systems.

Annexes

Annex A



Annex B

Materials	Values
Resistance	5 %
Coil	2 mh (4 A)
Alimentation	15 V
current sensor	10 A
voltage sensor	20 A

Annex C

P&O program

```
function D = PandO(V, I, Params)
```

```
    Dinit = Params(1);
```

```
    Dmax = Params(2);
```

```
    Dmin = Params(3);
```

```
    deltaD = Params(4);
```

```
    persistent Vold Pold Dold;
```

```
    dataType = 'double';
```

```
    if isempty(Vold)
```

```
        Vold=0;
```

```
        Pold=0;
```

```
        Dold=Dinit;
```

```
    End
```

```
        P= V*I;
```

```
        dV= V - Vold;
```

```
        dP= P - Pold;
```

```
        if dP ~= 0
```

```
            if dP < 0
```

```
                if dV < 0
```

```
                    D = Dold - deltaD;
```

```
                else D = Dold + deltaD;
```

```
            end
```

```
        else if dV < 0
```

```
            D = Dold + deltaD;
```

```
        else D = Dold - deltaD;
```

```
        end
```

```
    end
```

```
    else D=Dold;
```

```
    end
```

```
    if D >= Dmax | D<= Dmin
```

```
        D=Dold;
```

end

Dold=D;

Vold=V;

Pold=P;

end

Bibliographical References

[9]<https://www.google.com/search?q=cellule%20solaire&udm=2&sa=X&ved=0CCoQtI8BahcKEwjw1NzYnO6MAxUAAAAAHQAAAAAQBw&biw=1280&bih=593&dpr=1.5#vhid=8mNzGMHBtNP1aM&vssid=mosaic> (accessed on 04/04/2025)

[10]https://www.google.com/search?q=Principle+of+a+photovoltaic+cell.&sca_esv=a2fccd0347a25b28&rlz=1C1ONGR_frDZ1097DZ1097&udm=2&biw=1280&bih=593&sxsrf=AHTn8zpjUdFM460ebDi4x4D34aoFY49iQ%3A1745413688779&ei=OOYIaNmjL7eTkDUPstvQsQ8&ved=0ahUKEwjZn5_XnO6MAxW3SaQEHBltNPYQ4dUDCBI&uact=5&oq=Principle+of+a+photovoltaic+cell.&gs_l=EGNpbWciIVByaW5jaXBsZSBvZiBhIHBob3Rvdm9sdGFpYyBjZWxsLjIGEAAYBRgeSPovUNohWNohcAJ4AJABAJgBkAGgAZABqgEDMC4xuAEDyAEA-AEB-AECmAIDoAK6AagCCsICChAjGcCYyQIY6gKYAWiSBwMyLjGgB36yBwMwLjG4B5gB&sclient=img#vhid=N4bC167NSBISjM&vssid=mosaic (accessed on 04/10/2025)

[11] BOUDALI Nour El Houda, GUEBLI Sayeh Abdelazziz ,« Etude et Réalisation d'Un Système Photovoltaïque à Base d'Une Carte Arduino UNO », Mémoire de Master , Université Ibn-Khaldoun de Tiaret,2023.

[12]https://www.google.com/search?q=%3A+symbol+of+DCDC+converter+.&rlz=1C1ONGR_frDZ1097DZ1097&oq=%3A+symbol+of+DCDC+converter+.&gs_lcrp=EgZjaHJvbWUyBggAEEUYOTIICAEQABgWGB4yCAgCEAAyFhgeMgoIAXAAGIAEGKIEMgcIBBAAGO8FMgcIBRAAGO8FMgcIBhAAGO8F0gEJMTc2N2oxajE1qAIIsAIB8QXbWipe2MmuW_EF21iKXtjJrls&sourceid=chrome&ie=UTF-8#vhid=F-gki_ijuSlz6M&vssid=_Um9NaMjgL8jU7M8PvZH6kAY_40 (accessed on 04/10/2025)

[13][https://www.google.com/search?sca_esv=813765718ccf2407&rlz=1C1ONGR_frDZ1097DZ1097&sxsrf=AE3TifP24PAa5OFBupLvopOOvRO6vIf9w:1749551010705&q=Characteristic+Ppv\(Vpv\)+P%26O.&udm=2&fbs=AlljpHx4nJjfGojPVHhEACUHPiMQ_pbg5bWizQs3A_kIenjtcpTTqBUdyVgzq0c3_k8z34GUa4Q_jiUQNh5K5XfwsFj1JlsgDwnS6F9uJOn6Vp7K2HZtT5LU LhH94JKrGo2j1UnNL1DQzM7nSAtwSmn49vZJ9EsuwEPPLT1eZtmWAGYleSR7i8T6Ebysb1oqAZ33Y_e72BLEQvErZadNFT0gbRrwnesA&sa=X&ved=2ahUKEwjtqom00eaNAxW9XaQEHRrCC5IQtKgLegQIFRAB&biw=1280&bih=593&dpr=1.5#vhid=ulMKDMSMTek4OM&vssid=mosaic](https://www.google.com/search?sca_esv=813765718ccf2407&rlz=1C1ONGR_frDZ1097DZ1097&sxsrf=AE3TifP24PAa5OFBupLvopOOvRO6vIf9w:1749551010705&q=Characteristic+Ppv(Vpv)+P%26O.&udm=2&fbs=AlljpHx4nJjfGojPVHhEACUHPiMQ_pbg5bWizQs3A_kIenjtcpTTqBUdyVgzq0c3_k8z34GUa4Q_jiUQNh5K5XfwsFj1JlsgDwnS6F9uJOn6Vp7K2HZtT5LU LhH94JKrGo2j1UnNL1DQzM7nSAtwSmn49vZJ9EsuwEPPLT1eZtmWAGYleSR7i8T6Ebysb1oqAZ33Y_e72BLEQvErZadNFT0gbRrwnesA&sa=X&ved=2ahUKEwjtqom00eaNAxW9XaQEHRrCC5IQtKgLegQIFRAB&biw=1280&bih=593&dpr=1.5#vhid=ulMKDMSMTek4OM&vssid=mosaic) (accessed on 04/13/2025)

[14] GUENIF NOUR ALISLAM, DJOTNI ABDELKARIM, « Technique MPPT d'un système PV par le réseau de neurone », Mémoire de Master, Université Badji Mokhtar- Annaba, 2023.

[15] HARENDI Amine, ARBAOUI Ali, « Calcul de l'MPPT par réseaux de neurone pour un système photovoltaïque », Mémoire de Master, Université Kasdi Merbah Ouargla ,2015.

[16]https://www.google.com/search?sca_esv=5c548f5d6bb0e814&rlz=1C1ONGR_frDZ1097DZ1097&sxsrf=AHTn8zpj8bkxJD9VVUDU7Zc_s6e7jXq9czg:1745926289428&q=biological+neuron&udm=2&fbs=ABzOT_BnMAgCWdhr5zilP5f1cnRvJ3SHQcDVxkdpDyHwlRhdNfnoCIRh0PKqyvFYyTfIeCoWIR5C1jUN_wgcDJ8Cdwgf887IFxRCsZbfrfzJNeHIEy80VyFhnoKMrhh4XoEeE6uQpFGbb3E_i4luZ6at9xSdooGfXTwM21WbM8ValzBRU82u7sJ0jj5E0LVOTF190ksrj_WYCYiQljCGpXrlZujKA&sa=X&ved=2ahUKEwi_h6Sikv2MAxU3KvsDHRI7F2YQQtKgLegQIFxAB&biw=1280&bih=593&dpr=1.5#vhid=hCc2jFgumGJz5M&vssid=mosaic (accessed on 05/06/2025)

[17] Y.Mihoub, « Généralité sur les réseaux de neurones », polycopie, Université Ibn-Khaldoun de Tiaret.

[18] https://www.google.com/search?sca_esv=1708c7095128329f&rlz=1C1ONGR_frDZ1097DZ1097&sxsrf=AHTn8zp7qsVz3PqNbPG68e9wdsCqpK_TAQ:1745854140943&q=Artificial+neuron+model&udm=2&fbs=ABzOT_BnMAGCWdhr5zilP5f1cnRvJ3SHQcDVxkdpDyHwIRhdNfno-CIRh0PKqyvFYyTkfIeCoWIR5C1jUN_wgcDJ8CdwYzZb459Ji35mF6-Diw-MEVIbiVb9rEyScNmbWMEBtioBRihrcCSCFcWsJ1AVK331h3tVPQ6liURUHTEhOYH2gKVzNoDf2OAPDcoBUpW0VJNbuag02X6CNEX3A1yBGbLjel1w&sa=X&ved=2ahUKEwj85m_hfuMAxUHVkQEHVgfJvUQtKgLegQIExAB&biw=1280&bih=593&dpr=1.5#vhid=6pUcF7eFYp0g-M&vssid=mosaic (accessed on 05/18/2025)

[19] Mr.Mohammed Nadjib KHEMGANI ,Mr.Said BOULAGUESSA ,Mr.Abdellah DLILI « MPPT Solar Using ANN, FL and P&O via Buck converter », Academic Master Dissertation, University of Kasdi Merbah Ouargla,2024.

[20] <file:///D:/schema%20reseau%20non%20boucle-%20Recherche%20Google.html> (accessed on 05/19/2025)

[21] BEKHEDDA ABDERRAHMANE, BELMEKKI SOHEIL, « Détection de défauts dans un système photovoltaïque par l'intelligence artificielle », Mémoire de Master, Université Abdelhamid Ibn Badis Mostaganem, 2024.

[22] https://www.google.com/search?sca_esv=076e05d021dd9d5f&rlz=1C1ONGR_frDZ1097DZ1097&sxsrf=AHTn8zrndI36YqmhvNxn54czy8LoIppBnQ:1746006947568&q=figure+reseau+boulee&udm=2&fbs=ABzOT_BnMAGCWdhr5zilP5f1cnRvJ3SHQcDVxkdpDyHwIRhdNfnoCIRh0PKqyvFYyTkfIfJOoyi6rL2ScSJ67dNoiLlma6nffqoENgGX1QoQK1HAykFUAcq3rMZkdS_sg1VysuLhEuYXAo4SiCml1S8uvm2_uLVgmNycLE_mOOOwA3yhTWZAZVRfcR5Tf7MqaFZIRjNCTV7Fs1c0k2YrykkUV_DNiGg&sa=X&ved=2ahUKEwiHm4rfvvMAxVxKvsDHcb9EWgQtKgLegQIExAB&biw=1280&bih=593&dpr=1.5#imgcr=y52r5Z158EIMQM&imgdii=mih7rs6944XNvM (accessed on 05/23/2025)

[23] Guezzoun Nadia, Guezzoun Siham, « Techniques Intelligentes pour la Poursuite du Point de Puissance Maximale (MPPT) d'un Système Photovoltaïque », Mémoire de Master, UNIVERSITE ECHAHID HAMMA LAKHDAR-EL OUED ,2016.

[24] DJILALI BEIDA MAAMAR, « APPLICATION DE L'ALGORITHME GENETIQUE ET LES ELEMENTS FINIS A L'ETUDE DU COMPORTEMENT A L'ENDOMMAGEMENT DES COMPOSITES SOUMIS A L'IMPACT », Thèse de Doctorat, Université Abdelhamid Ibn Badis Mostaganem, 2017.

[25] Chahada, Brahim, « Analyse des données Electrocardiogramme par un système d'aide au diagnostic », Mémoire de Master , Abdel Hamid Ibn Badis University – Mostaganem, 2016.

[33] DEGUI Soumia, LARBI Sara, « Optimisation du contrôle MPPT des panneaux solaires avec la prise en compte de l'ombrage partiel », Mémoire de Master, Université Ibn-Khaldoun de Tiaret, 2024.

[34] Ressa.Noureddine, Merabet Leila, Omeiri Amar, « Perturb and Observation MPPT algorithm for the performance of Solar Photovoltaic System », Badji Mokhtar University 23000 Annaba, P.O Box 12, Algeria.

[35] HANANOU FATIHA, ROUABAH AICHA, « Modélisation et simulation d'un système photovoltaïque », Mémoire de Master, Université Kasdi Merbah Ouargla, 2014.

[36] Mr. OUARI Mondher et Mr. ZINE Yakoub, « Étude des commandes MPPT d'un système Photovoltaïque », Mémoire de Master, École nationale polytechnique, ENP 2020.

[37]https://www.google.com/search?sca_esv=a7528baf20b27cbb&rlz=1C1ONGR_frDZ1097DZ1097&sxsrf=AHTn8zpUTGcNy2DTCK6hdJFmktAspLx_LA:1744804496209&q=Solar+energy+conversion+chain+with+MPPT+control&udm=2&fbs=ABzOT_BnMAgCWdhr5zilP5f1cnRvJ3SHQcDVxkdpDyHwlRhdNfnoCIRh0PKqyvFYyTkfleCoWIR5C1jUN_wgcDJ8Cdwgf887IFxRCsZbfrfzJNeHIEy80VyFhnokMrhh4XoEeE6uQpFGbb3E_i4luZ6at9xSdoo-GfXTwM21WbM8-ValzBRU82u7sJ0jj5E0LVOTF190ksrj_WYCYiQljCGpXrlZujK-A&sa=X&ved=2ahUKEwj3xsuhv9yMAxWtRPEDHXykDuYQtKgLegQIExAB&biw=1280&bih=593&dpr=1.5#vhid=9HcG-7X7dbMzxM&vssid=mosaic (accessed on 06/05/2025)

[38] Houairi Said, Kerbouai Fouad, « Implémentation de la commande scalaire pour la machine asynchrone sous une carte DSPACE 1104 », Mémoire de Master, Université de Mohamed El-Bachir El-Ibrahimi - Bordj Bou Arreridj ,2022.

[39] Mr BEN BOUDAUD MOURAD, Melle MOKRANI Zahra, « Alimentation d'une machine asynchrone par onduleur MLI en utilisant la carte DSPACE 1104 », Mémoire de Master, Université Abderrahmane Mira de Bejaia, 2012.

ملخص

يركز هذا العمل في نهاية الدراسة على تقييم أداء الخوارزمية الجينية (GA) لمراقبة نقطة الطاقة القصوى (MPPT) في نظام كهروضوئي. والهدف من ذلك هو تحسين إنتاج الطاقة من خلال مقارنة هذه الطريقة الذكية مع الأساليب التقليدية مثل Perturb & Observe (P&O) والتقنيات الذكية الأخرى مثل الشبكات العصبية الاصطناعية (ANN)، خاصة في وجود تظليل جزئي. أُجريت عمليات محاكاة باستخدام Matlab/Simulink لتحليل سلوك الطرق الثلاث، ثم أُجريت تجربة معملية باستخدام لوحة DSPACE 1104 وطريقة P&O. أظهرت النتائج أن الخوارزمية الوراثية تقدم أفضل أداء من حيث سرعة التقارب والمتانة، مع تسليط الضوء على الحاجة إلى تحسين تنفيذها للتطبيقات في الوقت الحقيقي.

الكلمات المفتاحية: نظام كهروضوئي، خوارزمية جينية، تتبع نقطة الطاقة القصوى، اضطراب ومراقبة، شبكة عصبية اصطناعية، تظليل جزئي، بطاقة DSPACE 1104.

Abstract

This diploma thesis focuses on evaluating the performance of the Genetic Algorithm (GA) for Maximum Power Point Tracking (MPPT) in a photovoltaic system. The aim is to optimize energy production by comparing this intelligent method with conventional approaches such as Perturb & Observe (P&O) and other intelligent techniques such as artificial neural networks (ANN), particularly in the presence of partial shading. Simulations were carried out in Matlab/Simulink to analyze the behavior of the three methods, followed by laboratory experimentation using the DSPACE 1104 card and the P&O method. The results showed that the genetic algorithm offers the best performance in terms of convergence speed and robustness, while highlighting the need to optimize its implementation for real-time applications.

Keywords: Photovoltaic System ,Genetic Algorithm , Maximum Power Point Tracking , Perturb & Observe ,Artificial Neural Network , Partial Shading , DSPACE 1104 card.

Résumé

Ce travail de fin d'études porte sur l'évaluation des performances de l'algorithme génétique (AG) pour le suivi du point de puissance maximale (MPPT) dans un système photovoltaïque. L'objectif est d'optimiser la production d'énergie en comparant cette méthode intelligente à des approches classiques comme Perturb & Observe (P&O) et à d'autres techniques intelligentes comme les réseaux de neurones artificiels (RNA), notamment en présence d'ombrage partiel. Des simulations ont été réalisées sous Matlab/Simulink pour analyser le comportement des trois méthodes, puis une expérimentation a été menée en laboratoire à l'aide de la carte DSPACE 1104 avec la mise en œuvre de la méthode P&O. Les résultats ont montré que l'algorithme génétique présente les meilleures performances en termes de rapidité de convergence et de robustesse, tout en soulignant la nécessité d'optimiser sa mise en œuvre pour les applications en temps réel.

Mots clés : Algorithme Génétique, Système Photovoltaïque, Suivi du Point de Puissance Maximale, Perturb & Observe, Réseaux de Neurones Artificiels, Ombrage Partiel, Carte DSPACE 1104.